DUDLEY KNOX LIBRARY
NAVAL POSTGRADUATE SCHOOL
MONTEREY, CALIFORNIA 93943-5002

NAVAL POSTGRADUATE SCHOOL
Monterey, California

THESIS

N155

METALLIZED FUEL PARTICLE SIZE STUDY
IN A SOLID FUEL RAMJET

by

James Allen Nabity

September 1989

Thesis Advisor: David W. Netzer

Approved for public release; distribution is unlimited

REPORT DOCUMENTATION PAGE

Form Approved OMB No 0704-0188

1a REPORT SECURITY CLASSIFICATION: UNCLASSIFIED

1b RESTRICTIVE MARKINGS:

2a SECURITY CLASSIFICATION AUTHORITY:

2b DECLASSIFICATION / DOWNGRADING SCHEDULE:

3 DISTRIBUTION / AVAILABILITY OF REPORT: Approved for Public Release; Distribution is Unlimited

4 PERFORMING ORGANIZATION REPORT NUMBER(S):

5 MONITORING ORGANIZATION REPORT NUMBER(S):

6a NAME OF PERFORMING ORGANIZATION: Naval Postgraduate School

6b OFFICE SYMBOL (If applicable): 67

7a NAME OF MONITORING ORGANIZATION: Naval Postgraduate School

6c ADDRESS (City, State, and ZIP Code): Monterey, CA 93943-5000

7b ADDRESS (City, State, and ZIP Code): Monterey, CA 93943-5000

8a NAME OF FUNDING / SPONSORING ORGANIZATION:

8b OFFICE SYMBOL (If applicable):

9 PROCUREMENT INSTRUMENT IDENTIFICATION NUMBER:

8c ADDRESS (City, State, and ZIP Code):

10 SOURCE OF FUNDING NUMBERS

PROGRAM ELEMENT NO	PROJECT NO	TASK NO	WORK UNIT ACCESSION NO

11 TITLE (Include Security Classification): METALLIZED FUEL PARTICLE SIZE STUDY IN A SOLID FUEL RAMJET

12 PERSONAL AUTHOR(S): Nabity, James A.

13a TYPE OF REPORT	13b TIME COVERED	14 DATE OF REPORT (Year, Month, Day)	15 PAGE COUNT
Master's Thesis	FROM _____ TO _____	September 1989	63

16 SUPPLEMENTARY NOTATION: The views expressed in this thesis are those of the author and do not reflect the official policy or position of the Department of Defense or the U.S. Government.

17 COSATI CODES		
FIELD	GROUP	SUB GROUP

18 SUBJECT TERMS (Continue on reverse if necessary and identify by block number): Solid Fuel Ramjet, Combustion, Laser Particle Measurement, Metallized Fuel

19 ABSTRACT (Continue on reverse if necessary and identify by block number)

Particle size measurements were obtained at the grain exit and nozzle entrance in a solid fuel ramjet combustor using a boron based fuel. The particle size distributions at the aft end of the fuel grain were generally quadra-modal, with mode peaks at 2, 4, 15, and 25 - 45 microns. At the nozzle entrance the distributions were tri-modal, due to the complete oxidation of the 2 micron particles. $D_{3,2}$ and the size of the largest agglomerates increased with increasing equivalence ratio (or grain length), indicating that the longer grains result in more surface agglomeration. Combustion efficiency increased with equivalence ratio. A direct correlation of particle size alone with combustion efficiency was not obvious and may require an accurate measurement of particle concentration.

20 DISTRIBUTION / AVAILABILITY OF ABSTRACT: ☒ UNCLASSIFIED UNLIMITED ☐ SAME AS RPT ☐ DTIC USERS

21 ABSTRACT SECURITY CLASSIFICATION: UNCLASSIFIED

22a NAME OF RESPONSIBLE INDIVIDUAL: David W. Netzer

22b TELEPHONE (Include Area Code): (408)-646-2980

22c OFFICE SYMBOL: 67NT

DD Form 1473, JUN 86 — Previous editions are obsolete — S/N 0102-LF-014-6603

T245570

Approved for public release; distribution is unlimited

Metallized Fuel Particle Size Study
in a Solid Fuel Ramjet

by

James Allen Nabity
B.S., University of Nebraska-Lincoln, 1983

Submitted in partial fulfillment of the
requirements for the degree of

MASTER OF SCIENCE IN AERONAUTICAL ENGINEERING

from the

NAVAL POSTGRADUATE SCHOOL
September 1989

ABSTRACT

Particle size measurements were obtained at the grain exit and nozzle entrance in a solid fuel ramjet combustor using a boron based fuel. The particle size distributions at the aft end of the fuel grain were generally quadra-modal, with mode peaks at 2, 4, 15, and 25 - 45 microns. At the nozzle entrance the distributions were tri-modal, due to the complete oxidation of the 2 micron particles. $D_{3,2}$ and the size of the largest agglomerates increased with increasing equivalence ratio (or grain length), indicating that the longer grains result in more surface agglomeration. Combustion efficiency increased with equivalence ratio. A direct correlation of particle size alone with combustion efficiency was not obvious and may require an accurate measurement of particle concentration.

Thesis
N155
C.1

TABLE OF CONTENTS

I. INTRODUCTION.....1

A. INTEGRAL ROCKET RAMJET.....1

B. RAMJET COMBUSTION.....2

C. PARTICLE SIZE MEASUREMENT.....6

II. PROCEDURE.....9

A. COMBUSTOR CONFIGURATION.....9

B. NPS COMBUSTION LABORATORY.....11

C. TEST PROCEDURE.....11

D. TEST MATRIX.....14

E. PARTICLE SIZE MEASUREMENT.....15

1. Malvern Particle Sizer.....15

2. Alignment.....17

3. Particle Size Measurement Test Procedure....18

F. INSTRUMENTATION.....19

G. DATA ACQUISITION.....21

III. RESULTS.....22

IV. SUMMARY AND CONCLUSIONS.....33

LIST OF REFERENCES.....36

APPENDIX A (TEST 7).....38

APPENDIX B (TEST 9).....40

APPENDIX C (TEST 10).....42

MONTEREY, CALIFORNIA

APPENDIX D (TEST 11).....44

APPENDIX E (TEST 12).....46

APPENDIX F (TEST 13).....48

APPENDIX G (TEST 17).....50

INITIAL DISTRIBUTION LIST.....52

LIST OF TABLES

TABLE 1. TEST MATRIX FOR HTPB AND B_4C/HTPB FUELS.....15

TABLE 2. INSTRUMENTATION LIST.....20

TABLE 3. TEST RESULTS.....22

LIST OF FIGURES

Figure 1.1. Bypass-type, Solid-fueled, Integral Rocket Ramjet.....2

Figure 1.2. Basic Solid Fuel Ramjet Combustor and Important Characteristics.....3

Figure 1.3. Combustion and Flow Characteristics in the SFRJ Combustor.....4

Figure 2.1. SFRJ 2-½ Inch Direct-Connect Combustor.....9

Figure 2.2. Window Assembly.....10

Figure 2.3. NPS Subscale Ramjet Blowdown Facility.....12

Figure 2.4. B_4C Particle Size Distribution.....14

Figure 2.5. Malvern 2600 Particle Sizer.....16

Figure 2.6. Inlet/Combustor Instrumentation Locations....20

Figure 3.1. Light Diffraction Pattern.....25

Figure 3.2. Particle Size Distribution.....26

Figure 3.3. Particle Size Results (Volume Distribution)..28

Figure 3.4. Particle Size Results (Number Distribution)..29

Figure 3.5. Sauter Mean Diameter vs. Equivalence Ratio...30

Figure 3.6. Normalized Combustion Efficiency for B_4C/HTPB 31

LIST OF SYMBOLS

B_4C	Boron Carbide
$D_{3,2}$	Sauter Mean Diameter
F	Thrust
G	Vitiated Air Mass Flux
HTPB	Hydroxyl-terminated Polybutadiene
LFRJ	Liquid Fuel Ramjet
NPS	Naval Postgraduate School
P	Pressure
SFRJ	Solid Fuel Ramjet
T	Temperature
t_{psm}	Time (from ignition) of Particle Size Measurement
t_{res}	Mixing Section Residence Time
γ	Ratio of Specific Heats (C_p/C_v)
η	Normalized Combustion Efficiency
ϕ	Equivalence Ratio
$\dot{\omega}$	Mass Flow Rate

Subscripts

air	Vitiated Air
c	Combustor Chamber
f	Fuel
i	Inlet

p Purge Gas

3.1 Window Location at the Front End of the Mixing Chamber

3.2 Pressure Location at the Front End of the Mixing Chamber

3.3 Window Location at the Aft End of the Mixing Chamber

4.0 Pressure Location at the Aft End of the Mixing Chamber

I. INTRODUCTION

A. INTEGRAL ROCKET RAMJET

Solid fuel ramjet (SFRJ) propulsion has been proposed for air-to-air and air-to-surface missile applications. The ramjet concept is the simplest of all airbreathing engine cycles. However, a rocket boost is required to accelerate the missile to a minimum ramjet takeover velocity of about Mach 1.5 [Ref. 1:p. 4], since the ramjet doesn't produce any thrust at zero airspeed.

A sketch of a typical SFRJ integral rocket ramjet missile configuration is shown in Figure 1.1. The inlet diffuser slows the inlet air to subsonic speed, thereby increasing the static pressure. Combustion stability is provided by a flameholding mechanism (i.e. bluff body, sudden expansion, etc.) at the air inlet. Fuel from the walls mixes and burns with the inlet air and thrust is developed by expansion of the flow through the exhaust nozzle to supersonic velocities.

The solid fuel ramjet has no need for a fuel management system. Thus, the SFRJ has the advantage of a simpler and less expensive system than its liquid fueled (LFRJ) alternative. Yet, the performance of the SFRJ at certain equivalence ratios approaches that of the LFRJ. Although

relatively good performance has been demonstrated with hydrocarbon fuels, high energy metallized fuels have been developed that yield high combustion efficiency, while providing increased fuel loading because of higher density.

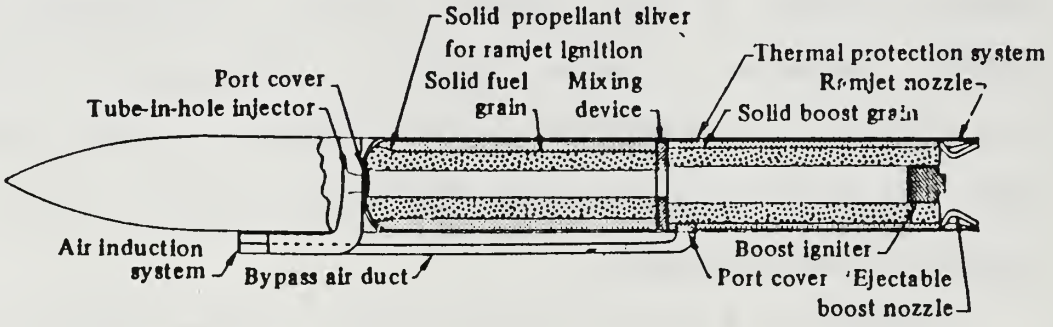

Figure 1.1. Bypass-type, Solid-fueled, Integral Rocket Ramjet [Ref. 1:p. 40]

B. RAMJET COMBUSTION

A flameholder is required in the combustor to stabilize the flame and is typically done by a sudden expansion from the inlet diffuser to the fuel grain, as indicated in Figure 1.2. Historically, an aft mixing chamber has been required to improve the overall combustion efficiency of the reacting fuel/air mixture. Bypass air is also used to improve mixing (thereby improving combustion efficiency) and reduce air flow through the fuel grain, which permits increased fuel loading.

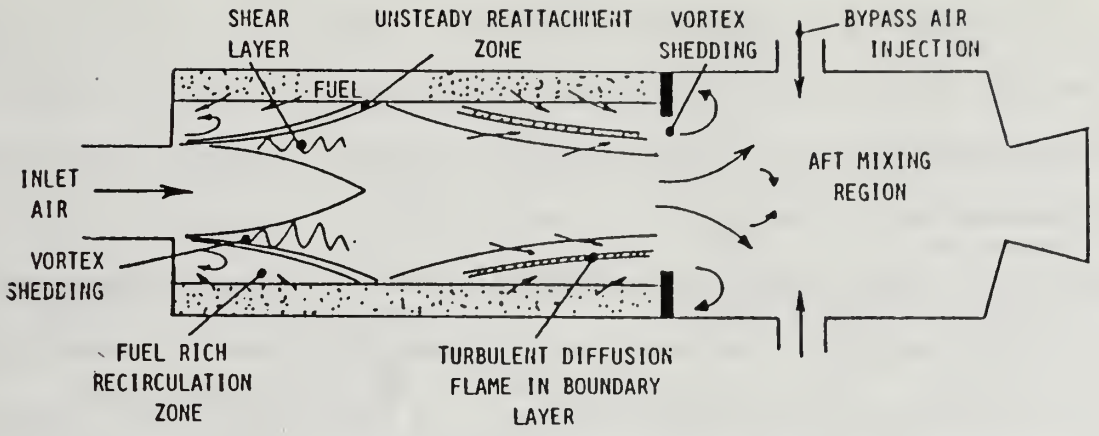

Figure 1.2. Basic Solid Fuel Ramjet Combustor and Important Characteristics [Ref. 2:p. 159]

A sketch of the combustion process that occurs for a non-metallized fuel is shown in Figure 1.3a. The combustion phenomena for non-metallized fuels are well understood [Refs. 4-6]. The fuel regression rate depends on the convective and radiative heat transfer from the gas-phase diffusion flame to the fuel surface. The diffusion flame is established in the turbulent boundary layer near the fuel surface [Ref. 4]. The regression rate is primarily a function of air mass flux and inlet air temperature.

The combustion phenomena are quite different for metallized fuels. Gany and Netzer [Refs. 2,3] describe the suspected combustion process for metallized fuels and this is sketched in Figure 1.3b. The radiative heat transfer has two sources in metallized fuel combustion: a weaker diffusion

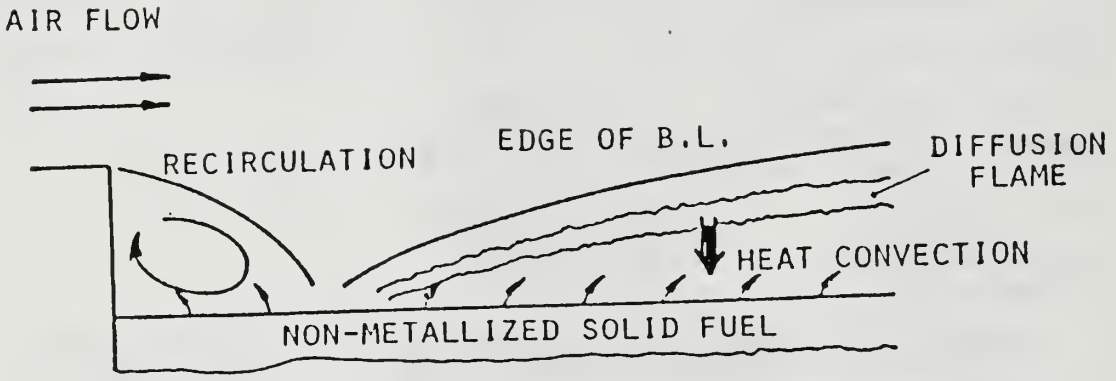

a) Nonmetallized Fuel

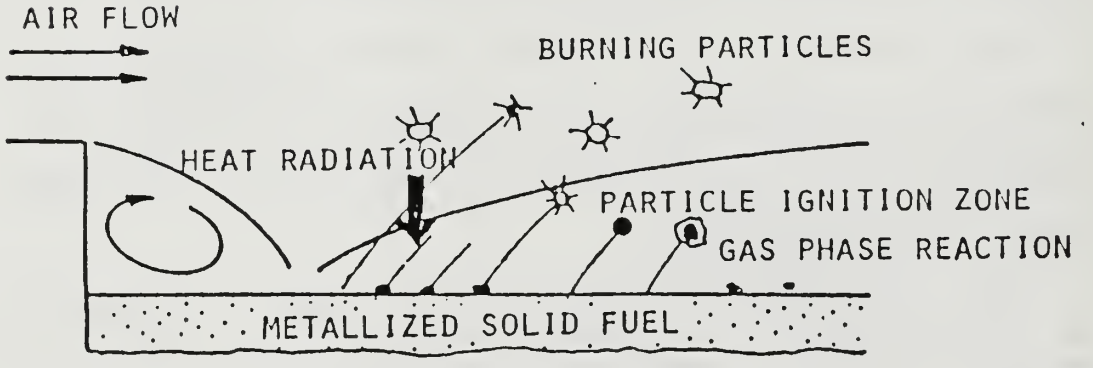

b) Metallized Fuel

Figure 1.3. Combustion and Flow Characteristics in the SFRJ Combustor [Ref. 3:p. 424]

flame (due to less hydrocarbon in the fuel) and the hot metal particles in the flow. The diffusion flame is expected to lie closer to the fuel surface. There is little or no oxygen at the fuel surface, hence, the metal particles can heat up, but will not ignite. In the combustion process the hydrocarbon vaporizes at the surface exposing the metal fuel particles. As more of the surrounding hydrocarbon fuel vaporizes the metal particles tend to coalesce before being ejected into the main flow. Ejection of the metal particles and agglomerates off of the fuel surface may be due to pressure forces or decomposition of the fuel surface with the help of cross-flow forces. A particle may collide with other particles and agglomerate and, if the particle gets hot enough (which depends upon the particle's size and trajectory), it will ignite when it comes in contact with the oxidizer. The agglomeration of metal particles may be one reason for poor combustion efficiency.

The oxide coating that surrounds the particle slows the rate of chemical reaction. Rapid oxidation of boron requires a gas temperature of about 1900 K [Ref. 7]. A finite combustor residence time is required for complete combustion and may be as much as 40 ms for a large agglomerate (50 μm) [Ref. 8:p. 43]. Since residence time is about 3 ms for an operational combustor, combustion efficiency may be poor.

Until recent years the combustion efficiency of metallized fuels (boron, magnesium, titanium, aluminum, etc.) had been poor. The use of additives has significantly improved the performance of some of these fuels, yet others still exhibit poor performance. The reason for the success of these additives with some fuels, but not all, is unclear. It is believed that the catalyst enhances the heat release near the surface. The oxide layer surrounding the metal particle reaches its boiling point sooner, so that the oxidizer can reach the metal particle and cause it to ignite.

C. PARTICLE SIZE MEASUREMENT

Measurement of the particle sizes and distribution at different locations in the combustor may provide insight into the combustion of metallized fuels and the resulting combustion efficiency. Researchers [Refs. 9,10] have used photographic methods to estimate particle size and distribution in the reacting flow environment of the solid fuel ramjet. Karadimitris [Ref. 9] took high speed movies of metallized fuel combustion in the recirculation zone and in the boundary layer region using a two-dimensional combustor setup. Paty [Ref. 10] utilized holography in a windowed, two-dimensional combustor to determine particle sizes near the fuel surface and in the gas stream. This technique was

limited to a resolution of about 20 μm, and most of the particles appeared to be smaller than this.

Particle size distributions need to be determined with a resolution of approximately 1-2 microns, if correlations with combustion efficiency are to be attempted. In addition, if it can be determined how the particle size distribution varies axially and radially through the combustor, then perhaps particle behavior can be related to measured combustion efficiency. Of course, the particle behavior can be expected to vary with combustor residence time, equivalence ratio, inlet air flow conditions, and fuel composition. Successful correlation of particle behavior with obtainable combustion efficiency should provide the information needed to better tailor fuel properties with flow conditions in order to optimize performance.

For particles larger than 1 micron, forward light diffraction measurements have been effective in determining particle size distribution [Ref. 11]. The Malvern Particle Sizer [Ref. 12] is one instrument which can provide particle size distributions for ensembles of particles.

The objective of this investigation was to measure the axial variation of the particle size distribution for boron-based solid fuels under different flow environments and to determine if measured performance could be correlated with the

particle behavior. Two-dimensional SFRJ combustors cannot be used to obtain meaningful combustion efficiency measurements. Therefore, an axisymmetric combustor configuration was employed.

II. PROCEDURE

A. COMBUSTOR CONFIGURATION

Solid fuel ramjet tests were conducted at the Naval Postgraduate School Combustion Laboratory. A subscale 2-½ inch, coaxial dump, axisymmetric combustor configuration, as shown in Figure 2.1, was tested in the direct-connect mode.

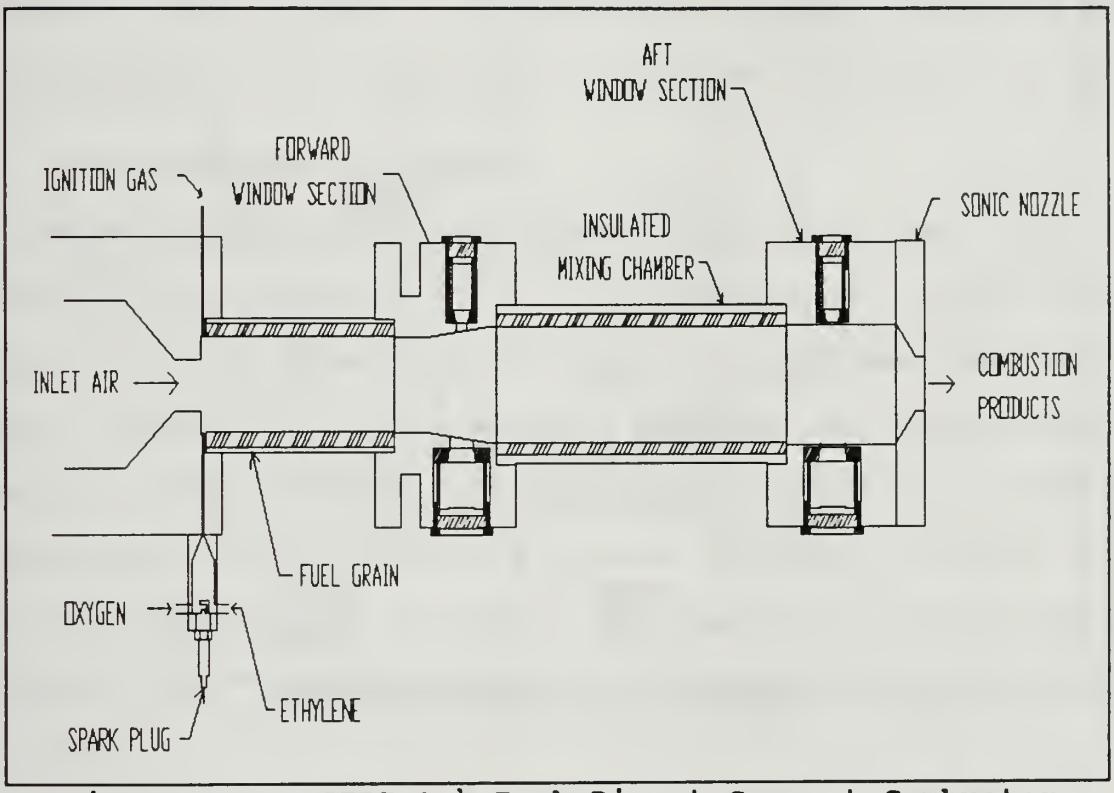

Figure 2.1. SFRJ 2-½ Inch Direct-Connect Combustor

The fuel grain was bolted between the inlet and the aft mixing chamber. The mixing chamber was insulated with DC93-104[1] to reduce heat loss through the combustor wall. A sonic nozzle (with graphite insert) bolts onto the aft mixing chamber.

A blowup of the window assembly can be seen in Figure 2.2. The laser beam passes through a fused silica window, which is

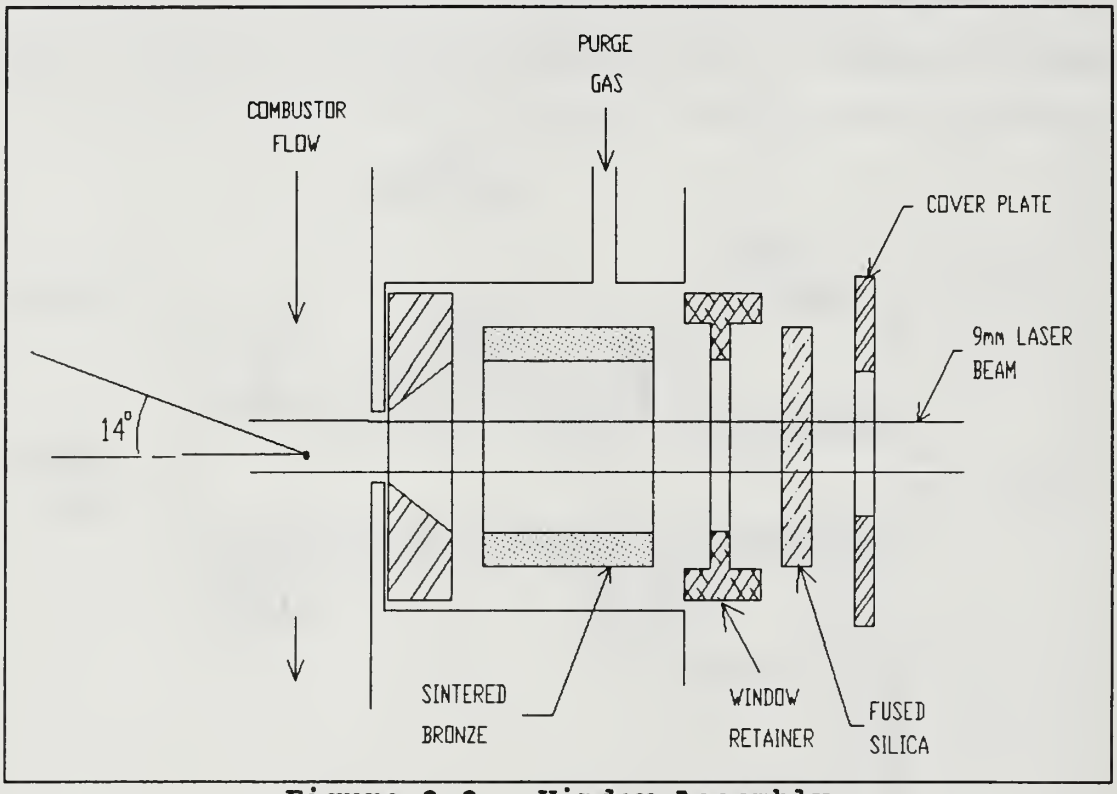

Figure 2.2. Window Assembly

[1]Dow Corning product with good high temperature characteristics. It is an ablative material that begins to char in the temperature range from 700 - 1400 F, and reaches a hard char at 1600 - 2500 F, forming a heat resistant barrier [Ref. 13:p. 23].

held in place by a retainer. The windows were kept clean during the combustion test by the purge gas (air) flowing through the sintered bronze, keeping the window chamber free of combustion products. From 5 - 10% of the total mass flow was required as purge gas, with more purge needed at the higher equivalence ratios, yet the largest window was still difficult to keep clean. The openings at each side of the test section were only large enough for the beam and scattered light to pass through. Stainless steel inserts plugged the window chambers for tests when the windows were not required.

B. NPS COMBUSTION LABORATORY

The facility has been discussed previously [Ref. 10]. A schematic of this facility is shown in Figure 2.3. Air flows from the high pressure (3000 psia) air storage through a choked nozzle to an air heater. Methane and ethylene were used as fuels for the air heater and oxygen was injected downstream of the heater to ensure that the vitiated air contained 23% oxygen by mass. The heater was acoustically isolated from the ramjet combustor with a sonically choked orifice.

C. TEST PROCEDURE

Air was bypassed to the atmosphere until the heater temperature had stabilized. At this time air was switched to

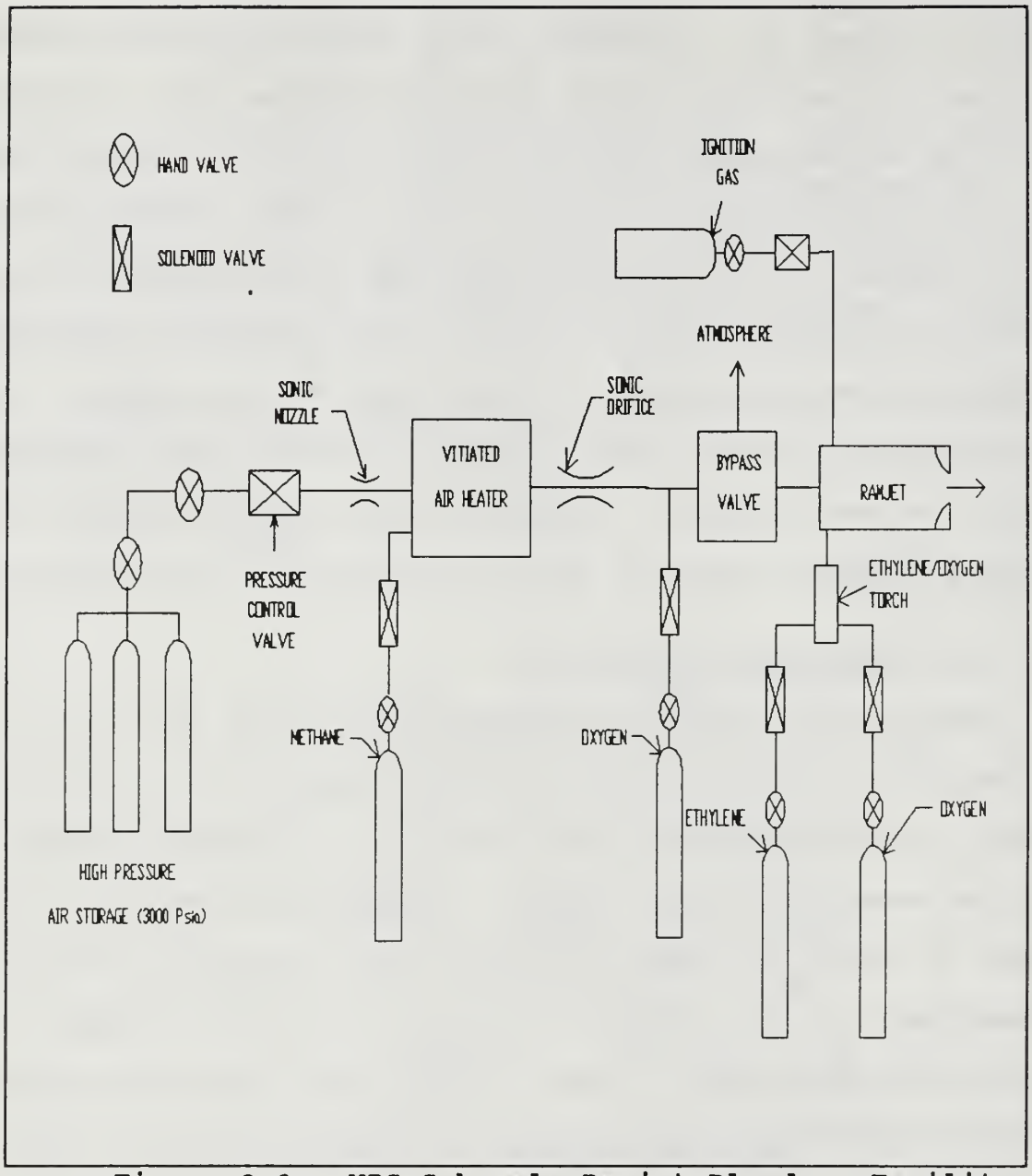

Figure 2.3. NPS Subscale Ramjet Blowdown Facility

the combustor, initiating a computer controlled sequence of events in which the fuel grain was preheated about 4 seconds, the ramjet combustor was ignited and sustained for the desired

burn time, and finally quenched at the end of the test. The air heater was secured immediately after the burn ended. The ethylene/oxygen torch ignited the ignition gas (ethylene) which in turn ignited the ramjet fuel grain. Approximately a one second ignition time was required for good ignition. Argon was used to quench the metallized fuel and nitrogen was used to quench the hydroxyl-terminated polybutadiene (HTPB) fuel.

HTPB (an all hydrocarbon fuel) and boron carbide/HTPB (a highly loaded metallized fuel) were used as solid fuel ramjet fuels. Both fuels were supplied by the Naval Weapons Center, China Lake, CA. HTPB was the baseline fuel for performance comparisons. The boron carbide (B_4C) particles used in the metallized fuel were manufactured by the Norton Company and had a nominal size distribution as shown in Figure 2.4. The Sauter mean diameter for these particles was about 9 microns.

The nozzle throat diameter was sized to maintain a nominal combustion pressure of 100 psia for all test conditions. The desired equivalence ratio was obtained by cutting the fuel grain to the appropriate length. The required fuel grain length at an initial port mass flux of 0.5 lbm/in^2-sec ranged from 3 inches (ϕ = .2) to 13.0 inches (ϕ = 1.0). The fuel grains had a nominal initial port diameter of 1.7 inches.

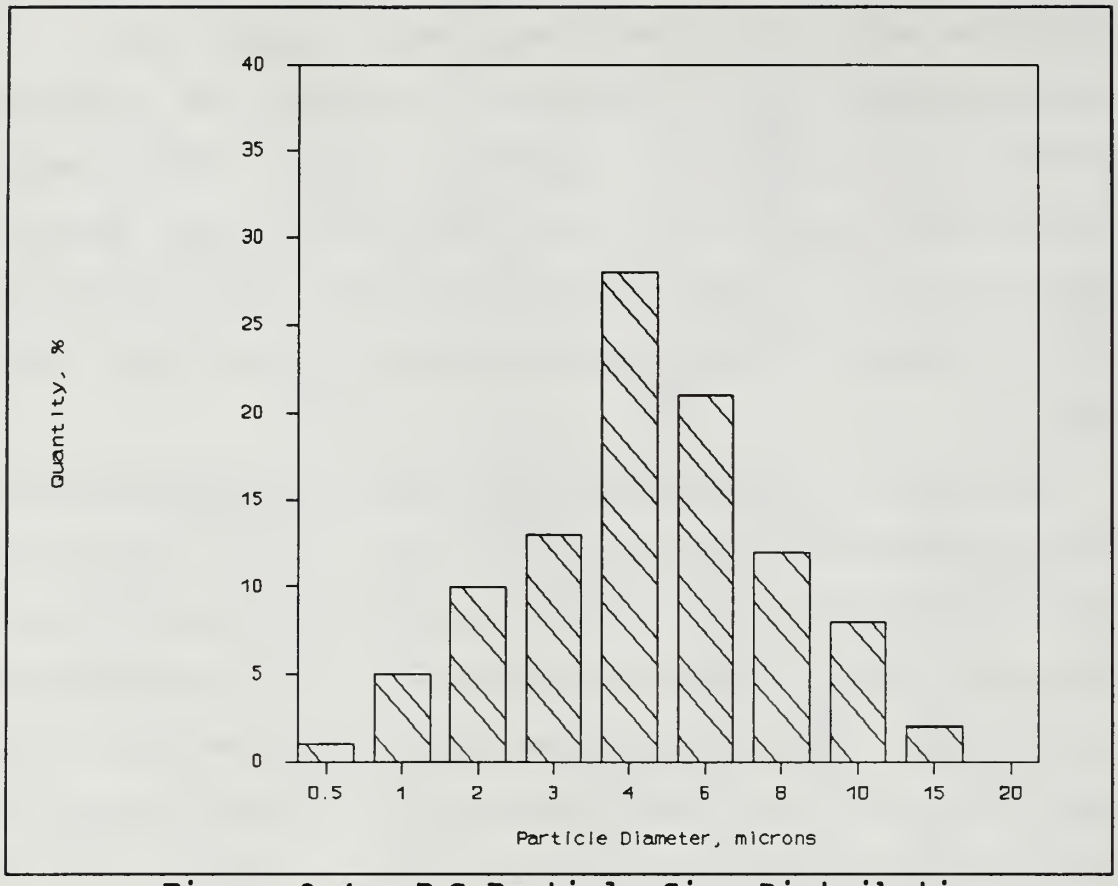

Figure 2.4. B_4C Particle Size Distribution

D. TEST MATRIX

The desired combustion test matrix is presented in Table 1. Due to delays in combustor fabrication, only tests with $G = .5$ lbm/in^2-s, $T_i = 1400$ R and $P_c = 100$ psia were conducted. Three tests were conducted with the metallized fuel at each condition. One test was for performance determination, one for particle size sampling at the forward end of the mixing chamber (station 3.1), and one for particle size sampling at the aft end of the mixing chamber (station 3.3).

TABLE 1. TEST MATRIX FOR HTPB AND B_4C/HTPB FUELS

G lbm/in^2-sec	ϕ	P_c psia	T_i deg R	Comment
.5	.2	100	1400	*
↓	.4	↓	↓	
↓	.6	↓	↓	*
↓	.8	↓	↓	
↓	1.0	↓	↓	*
↓	.4	60	↓	
↓	↓	100	1000	
.2	↓	↓	1400	*
.8	↓	↓	↓	
1.0	↓	↓	↓	*

* These conditions not tested with HTPB fuel

E. PARTICLE SIZE MEASUREMENT

1. Malvern particle sizer

Particle size measurements were made with a Malvern particle sizer (Model 2600 HSD). A schematic of the Malvern system is presented in Figure 2.5.

A 2mW He-Ne laser produced a collimated, monochromatic beam of light that illuminated the particles. The incident light was diffracted by the particles to give a stationary diffraction pattern independent of particle position and velocity. The instantaneous size distribution depended on the diffraction pattern. The Malvern 2600 Particle Sizer is based on far-field, near-forward Fraunhofer light diffraction. With a continuous flux of particles (supplied by the combustor) a

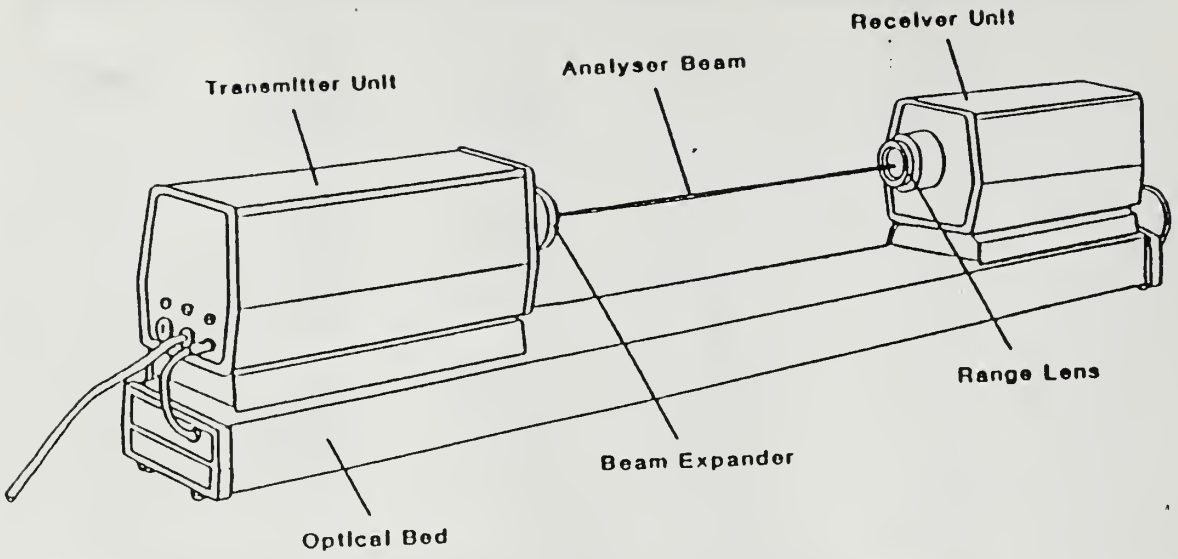

Figure 2.5. Malvern 2600 Particle Sizer [Ref. 12]

suitable number of samples (sweeps) were recorded and averaged to yield a final "measured" diffraction pattern. Typically, 50 sweeps were sufficient for a good average with a single sweep requiring about 7 msec for data collection.

The scattered light was focused onto a multi-element, photo-electric detector by a Fourier transform lens. The scattered light was measured at 31 discrete angles using concentric annular diodes. The photo-electric detector produced an analog signal proportional to the incident light intensity. An IBM/AT computer was interfaced to the detector and performed the integrations digitally.

The background scattered light was measured prior to the combustion test with cold air flowing through the

combustor. These voltages were subtracted from those obtained during the combustion test with particles present. In addition, the transmitted light was measured during the cold flow and ramjet combustion tests. These data were used to determine if multiple scattering effects were present and to determine the particle concentration according to Beer's Law.

The Malvern-provided software performs a non-linear least squares fit to the diffraction pattern to find the size distribution which gives the closest fit between the measured intensity profile and the theoretical profile expected from Fraunhofer diffraction. Multi-modal particle distributions were determined by this method. It was assumed that the particles could be separated into 32 discrete size bands. Particle sizes from 1.9 - 188 microns were measured in this way. [Ref. 12]

2. Alignment

Alignment of the Malvern 2600 particle sizer required care. A bandpass filter that blocked sunlight, while allowing the laser beam and scattered light to pass through, was placed over the lens. Reflections between the filter and the lens were minimized by rotating the filter while the Malvern system was in the align mode. Best results were achieved with the filter mounted directly on the lens.

The combustor test section was then mounted. Secondary reflections from the fused silica windows were difficult to eliminate. Rotating the combustor window section about 3 degrees was sufficient to place the reflected beams off of the ring diode. The windows were parallel to each other in the test section. A better method would have been to cock the windows relative to each other in order to prevent reflected light from striking the diode.

3. Particle Size Measurement Test Procedure

The ramjet combustion test procedure was modified slightly for tests during which a particle size measurement was taken. The window purge gas was activated just before the vitiated air was switched to the combustor. In the initial procedure, the window purge gas was left on for the duration of the test and was not shut off until after a post test measurement (to determine if window contamination occurred) had been made. After review of tests using this procedure it was determined that beam steering was caused by the interaction of the cold air window purge with the hot combustor flow.

Another procedure was developed in which the window purge gas was stopped immediately before particle size data was to be obtained. A measurement sample was then acquired and the window purge was reactivated to prevent destruction

of the windows. A post test measurement was taken to compare with the original background measurement as an indicator of fouled windows. Beam steering was significantly reduced, making this the preferred procedure, even though some uncertainty existed as to how much window contamination had occurred at the time of the measurement.

It was desirable to take more than one particle size measurement during a test. However, a limitation in the Malvern-provided software prevented this. High obscurations of 60 - 98% were observed during combustion tests. This high obscuration activated an alarm which locked the computer for up to eight seconds. The total combustor burn time was only about nine seconds. Thus, one measurement was taken about 3 - 5 seconds after ramjet ignition.

F. INSTRUMENTATION

Instrumentation for determining combustor performance consisted of combustor static pressure, inlet air temperature, flow rates and thrust measurements. The location of the static pressure taps in the inlet and combustor are displayed in Figure 2.6 and a complete list of instrumentation is provided in Table 2.

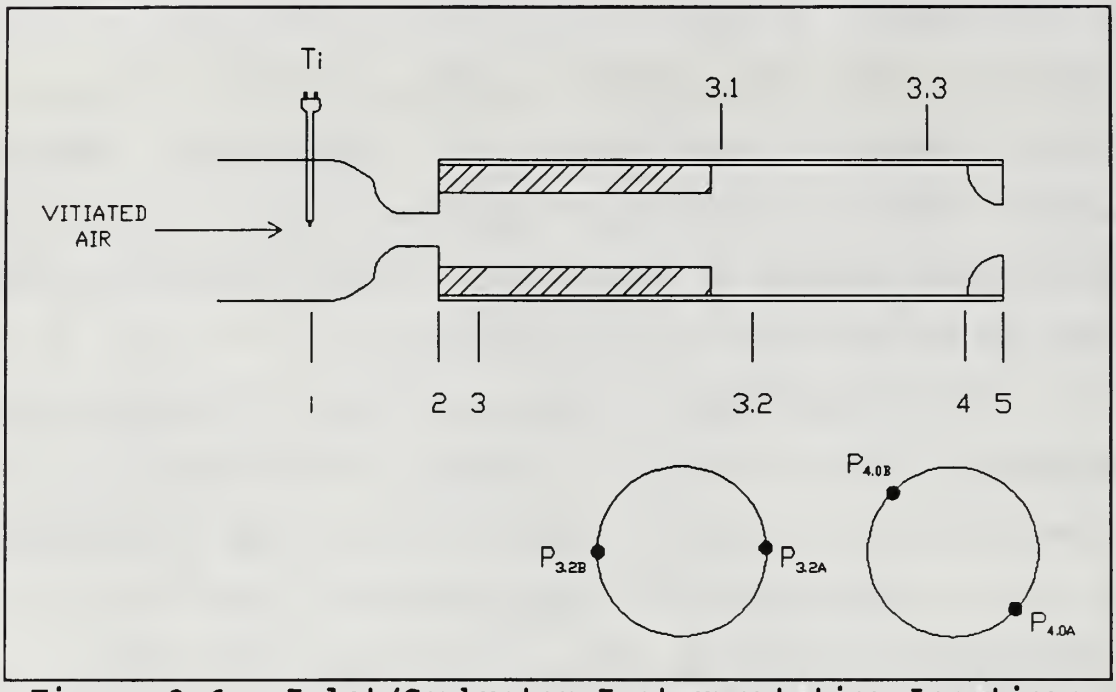

Figure 2.6. Inlet/Combustor Instrumentation Locations

TABLE 2. Instrumentation List

Pair	Air total pressure (0 - 2000 psig)
Pheater	Heater pressure (0 - 500 psig)
PO_2	Oxygen total pressure (0 - 1000 psig)
Pp	Window purge gas pressure (0 - 500 psig)
PCH_4	Heater gas pressure (0 - 2000 psig)
PC_2H_6	Ignition gas pressure (0 - 500 psig)
P_i	Inlet static pressure (0 - 200 psig)
$P_{3.2A}$	Combustor static pressure (0 - 500 psig)
$P_{3.2B}$	" " " " " "
$P_{4.0A}$	" " " (0 - 200 psig)
$P_{4.0B}$	" " " (0 - 500 psig)
Tair	Air temperature (type K)
TO_2	Oxygen temperature (type K)
T_p	Window purge gas temperature (type K)
TCH_4	Heater gas temperature (type K)
TC_2H_6	Ignition gas temperature (type K)
T_i	Inlet air temperature (type K)
F	Thrust (0 - 500 lbf)

G. DATA ACQUISITION

Data acquisition, reduction, and system control were achieved with a Hewlett-Packard 3054A system. Data was sampled and stored every .5 seconds for post test analysis. Primary components in the system were a HP-9836S computer, a HP-3497A data acquisition and control unit and a HP-3456A A/D integrating voltmeter. In addition, analog traces of chamber pressure and thrust were recorded. The analog record also located the exact time of the particle size measurement.

III. RESULTS

Seventeen tests were conducted and the steady state data are tabulated in Table 3. Air mass flux, inlet air temperature, combustion pressure, and combustor residence time were held approximately constant for these tests. Combustor residence time varied from 3 to 5 msec during these tests, but other data have indicated that little improvement in combustion efficiency occurs after 3 or 4 msec. Equivalence ratio and combustor flow Mach number were the only variables.

TABLE 3. TEST RESULTS

Test	Fuel	$\dot{\omega}_{air}$ lbm/s	$\dot{\omega}_f$ lbm/s	$\dot{\omega}_p$ lbm/s	ϕ	G lbm/in^2-s	T_i deg R	γ_i
1	HTPB	1.13	.029	0	.369	.486	1148	1.361
2	"	1.13	.031	0	.392	.480	1184	1.357
3	B_4C/HTPB	1.16	.047	.013	.402	.496	1254	1.353
4	"	1.13	.048	.028	.423	.482	1301	1.350
5	"	1.14	.050	.031	.428	.490	1302	1.349
6	"	1.13	.051	.049	.441	.483	1443	1.342
7	"	1.12	.054	.061	.466	.482	1272	1.354
8	"	1.12	.121	.065	1.03	.476	1231	1.357
9	"	1.10	.116	.086	.992	.466	1251	1.356
10	"	1.09	.087	.089	.744	.467	1266	1.355
11	"	1.10	.083	.092	.704	.468	1217	1.358
12	"	1.11	.069	.083	.585	.475	552	1.400
13	"	1.11	.047	.081	.399	.475	1210	1.358
14	"	1.12	.048	0	.430	.487	1219	1.358
15	"	1.12	.118	0	1.07	.474	1228	1.357
16	"	1.08	.084	0	.782	.469	1239	1.356
17	"	1.10	.047	.092	.395	.472	1217	1.358

TABLE 3. CONTINUED

Test	P_4 psia	P_{t4} psia	γ_4	γ_5	M_4	D_5 in	C_d	η	t_{res} msec	t_{psm} msec
1	149	150	1.284	1.322	.112	.977	.992	.87	4.4	*
2	102	104	1.280	1.309	.173	1.21	.994	1.0	4.0	*
3	107	109	1.259	1.267	.168	1.20	.993	.79	4.4	*
4	105	107	1.259	1.263	.168	1.19	1.00	.75	4.4	**
5	107	109	1.258	1.263	.172	1.19	1.02	.76	4.3	**
6	110	112	1.260	1.260	.168	1.19	1.00	.77	4.3	***
7	105	107	1.259	1.260	.171	1.19	1.02	.70	4.3	3
8	141	144	1.234	1.239	.172	1.20	1.01	.96	3.4	***
9	106	110	1.234	1.236	.234	1.38	1.02	1.05	3.2	8.8
10	94.5	97.6	1.241	1.245	.228	1.38	1.00	.84	3.7	****
11	93.0	96.2	1.243	1.245	.236	1.37	1.04	.91	3.5	2.8
12	92.3	96.5	1.250	1.250	.227	1.37	1.01	.97	3.7	2.5
13	103	105	1.261	1.270	.168	1.18	1.02	.67	4.6	3.5
14	103	105	1.260	1.265	.161	1.17	.991	.67	4.7	*
15	103	106	1.234	1.238	.227	1.37	1.00	1.00	3.3	*
16	89.1	92.0	1.239	1.245	.226	1.37	.997	.86	3.6	*
17	94.7	96.6	1.262	1.270	.177	1.21	1.02	.58	4.5	2.8

* Malvern 2600 not used
** Improper alignment
*** Lost data
**** Particle size measurement made as combustion ended

The first two tests were facility and instrumentation checkout tests using HTPB as the ramjet fuel. The remaining tests were with B_4C/HTPB metallized fuel. Tests 3 - 6 were required to verify both the ability of the window purge to keep the windows clean during the combustion test and whether proper beam alignment was maintained. It was determined from these tests that merely reducing the intensity level of reflected light on the diode was not good enough. The reflections had to be diverted off of the diode, such that no reflected light could strike the diode during a test.

Tests 7 - 13 were conducted with the Malvern system at one of two test locations (station 3.1 or station 3.3 as shown in Figure 2.6). During these tests particle size measurements were made with the window purge gas flowing. Test 17 was conducted using the preferred window purge procedure described previously. Although the diffracted light pattern was somewhat different for tests 7 and 17, the particle size distributions were nearly identical, as shown in Figures 3.1 and 3.2. Beam steering was evident on the first three diode rings. This data was suppressed before the particle size distribution was calculated. Elimination of the inner ring measurements will bias the results only if very large particles (> 50 μm) are present. Finally, tests 14 - 16 were conducted for performance data only.

Malvern Instruments MASTER Particle Sizer M6.10 Date 28-09-89 Time 13-57

Source test7 Record 2
Focal length 100

0	0.64	16	789.96
1	306.09	17	546.76
2	521.98	18	826.02
3	475.54	19	692.26
4	359.67	20	441.08
5	412.10	21	419.98
6	481.87	22	515.98
7	541.59	23	623.67
8	596.52	24	720.61
9	397.37	25	844.96
10	742.90	26	822.49
11	627.67	27	731.35
12	421.06	28	482.60
13	326.73	29	437.14
14	520.82	30	506.42
15	696.81	31	585.25

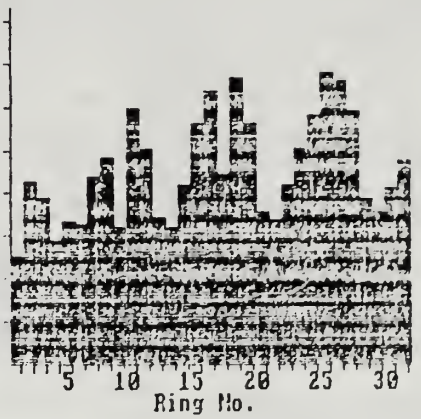

System number 2048 Diode DR487

a) Test 7

Malvern Instruments MASTER Particle Sizer M6.10 Date 23-09-89 Time 15-44

Source test17 Record 1
Focal length 100

0	0.96	16	265.18
1	365.18	17	230.94
2	177.05	18	261.81
3	107.24	19	221.25
4	87.64	20	218.39
5	115.50	21	252.04
6	141.39	22	277.77
7	176.37	23	298.43
8	215.09	24	303.89
9	220.54	25	345.34
10	161.73	26	330.21
11	108.38	27	304.45
12	114.69	28	307.97
13	147.63	29	314.87
14	194.99	30	327.24
15	245.75	31	318.22

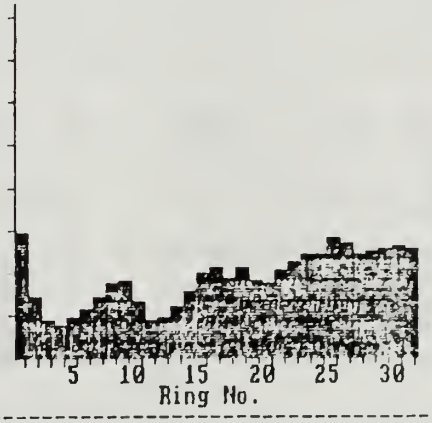

System number 2048 Diode DR487

b) Test 17

Figure 3.1. Light diffraction pattern

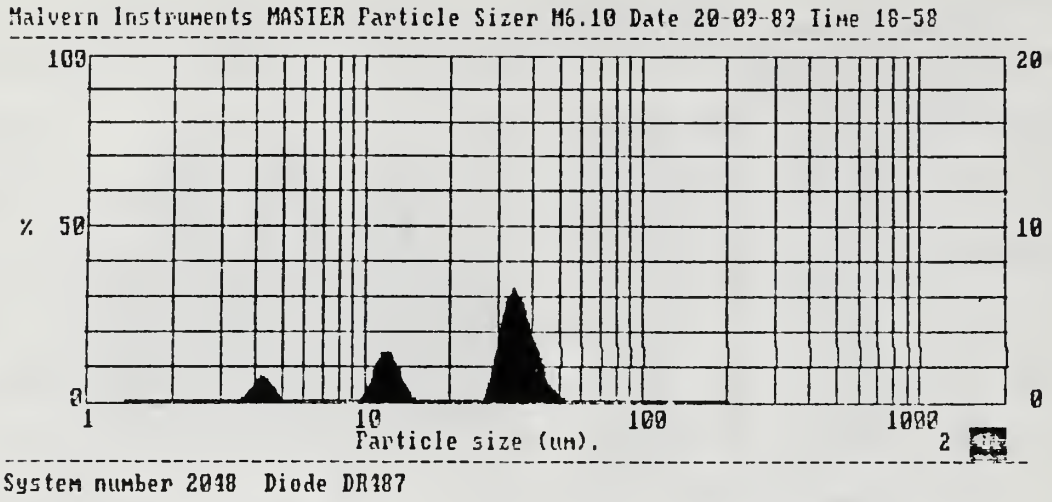

a) Test 7

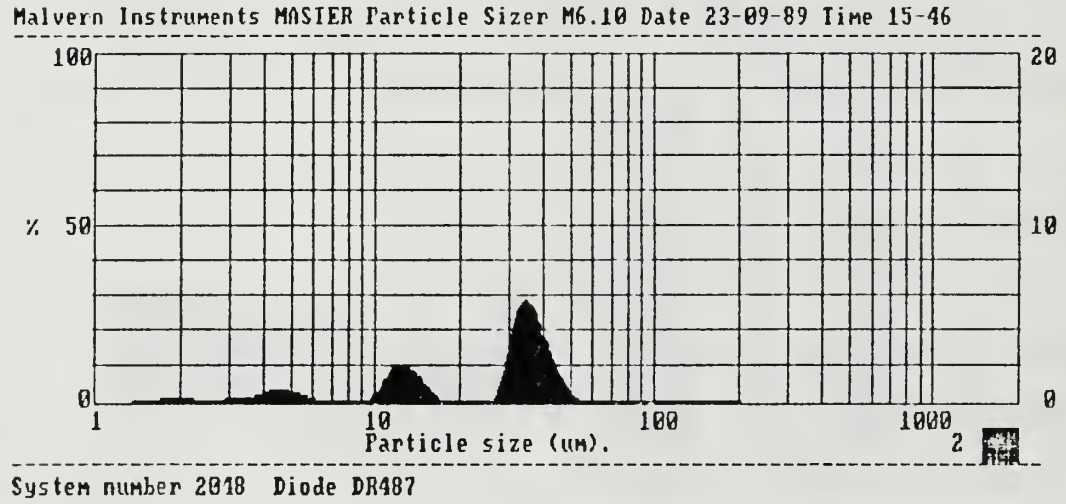

b) Test 17

Figure 3.2. Particle Size Distribution

Particle size distributions (volume and number basis) for tests 7 - 13, and 17 are included in the Appendix. A summary of this data is presented in Figures 3.3 (volume distribution) and 3.4 (number distribution).

Some general observations can be made from the particle size data in Figures 3.3 and 3.4. The particle size distributions were typically quadra-modal with peaks at approximately 2, 4, 15, and 25 - 45 microns. $D_{3,2}$ increased with increasing equivalence ratio. See also Figure 3.5. $D_{3,2}$ was constant across the mixing chamber, since smaller particles were consumed (which increased $D_{3,2}$) and larger particles were partially consumed (which decreased $D_{3,2}$).

The largest particles that were present must have been formed from the surface agglomeration of small particles, since the largest particle diameter in the fuel was 20 microns. The mean diameter for these large agglomerates increased from 34 to 45 microns with increasing equivalence ratio. This result may indicate that the longer fuel grains permit more agglomeration due to particle motion along the fuel surface.

A comparison of particle sizes and their respective masses and numbers at stations 3.1 and 3.3 indicated that the smallest particles (<2 μm) were consumed in the combustion process, as expected with burning time requirements of less than 2 msec [Ref. 8]. Some of the largest particles appeared

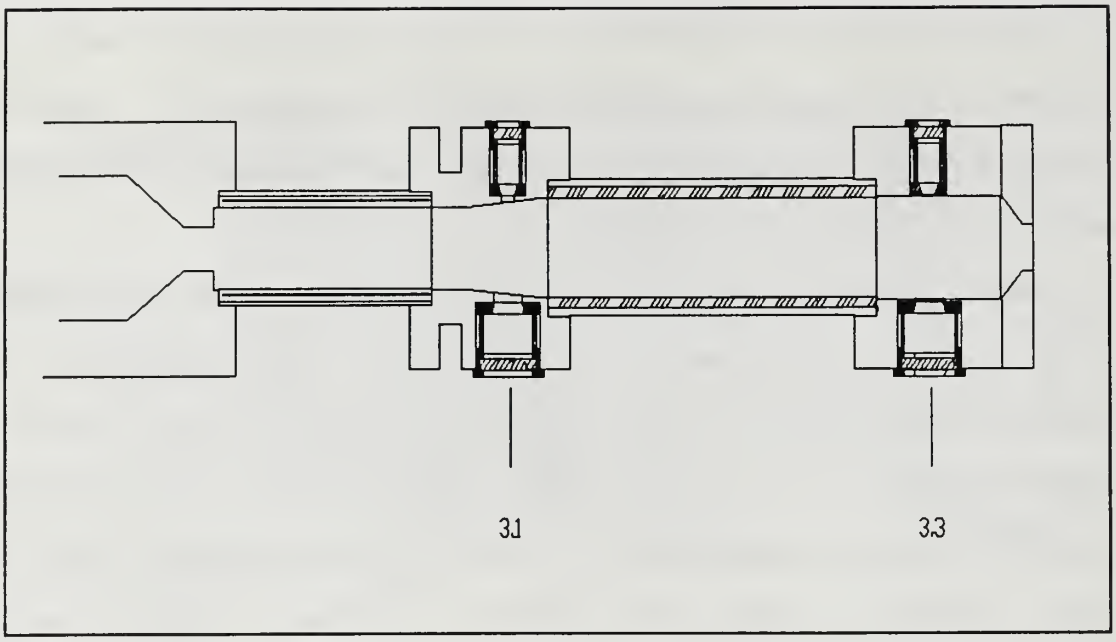

$P_c \simeq 100$ psia
$T_i \simeq 1230$ R
$G \simeq .5$ lbm/in^2-sec
$t_{res} \simeq 4$ msec

		Station 3.1		Station 3.3	
TEST	ϕ	$D_{3,2}$, μm	Peaks, μm	$D_{3,2}$, μm	Peaks, μm
7	.466	18	$<2_0$, 4_9, 12_{23}, 34_{68}	18	$<2_0$, 4_4, 9_{17}, 25_{79}
13	.399				
17	.395	17	$<2_2$, 4_9, 13_{23}, 34_{66}		
10	.744	22	$<2_1$, 4_7, 15_{25}, 45_{67}	20	$<2_0$, 4_9, 15_{25}, 42_{66}
11	.704				
9	.992	23	$<2_1$, 5_6, 15_{24}, 45_{69}		

Example: Test 7 (ϕ = .466)
$D_{3,2}$ = 18 μm
Peaks at 4, 12, and 34 μm
9% of the mass is distributed at 4 μm

Figure 3.3. Particle Size Results (Volume Distribution)

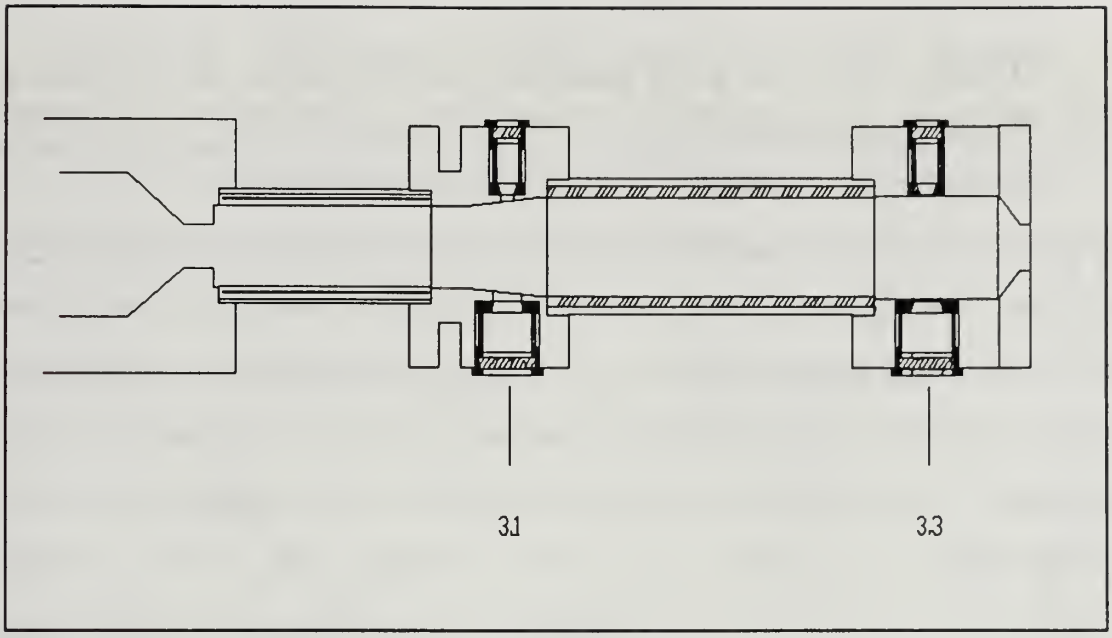

$P_c \simeq 100$ psia
$T_i \simeq 1230$ R
$G \simeq .5$ lbm/in^2-sec
$t_{res} \simeq 4$ msec

		Station 3.1		Station 3.3	
TEST	ϕ	$D_{3,2}$, μm	Peaks, μm	$D_{3,2}$, μm	Peaks, μm
7	.466	18	$<2_0$, 4_{87}, 12_{11}, 34_0	18	$<2_0$, 4_{75}, 9_{20}, 25_5
13	.399				
17	.395	17	$<2_{90}$, 4_9, 13_{11}, 34_0		
10	.744	22	$<2_{76}$, 4_{22}, 15_2, 45_0	20	$<2_0$, 4_{93}, 15_6, 42_1
11	.704				
9	.992	23	$<2_{79}$, 5_{19}, 15_2, 45_0		

Example: Test 7 (ϕ = .466)
$D_{3,2}$ = 18 μm
Peaks at 4, 12, and 34 μm
87% of particles are distributed at 4 μm

Figure 3.4. Particle Size Results (Number Distribution)

to either break up into smaller particles or be consumed at the lean equivalence ratios. In addition, most of the mass

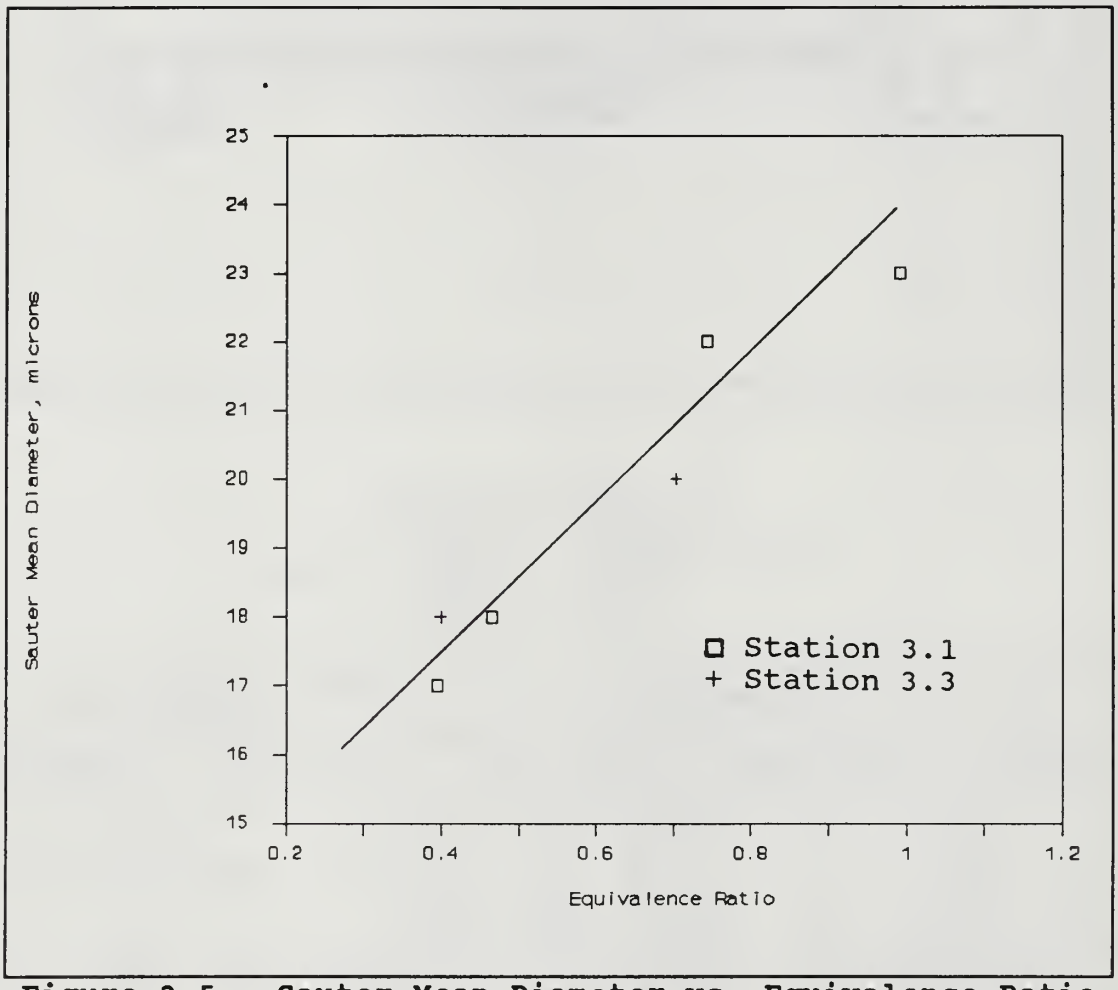

Figure 3.5. Sauter Mean Diameter vs. Equivalence Ratio

of unburned particles was concentrated in the largest particles, which are few in number. These particles passed through the mixing chamber without being completely oxidized, as expected for the short residence times in that region.

From the normalized combustion efficiency plotted in Figure 3.6, combustion efficiency is observed to increase with increasing equivalence ratio. In this figure, all temperature rise combustion efficiencies were determined from the static combustor pressure at station 4.0 and normalized by the combustion efficiency at ϕ = 1.0. Cold window purge air was seen to possibly increase combustion efficiency through forced mixing of oxygen with hot boron carbide particles. This may indicate that hot bypass air may result in significant improvement in combustion efficiency.

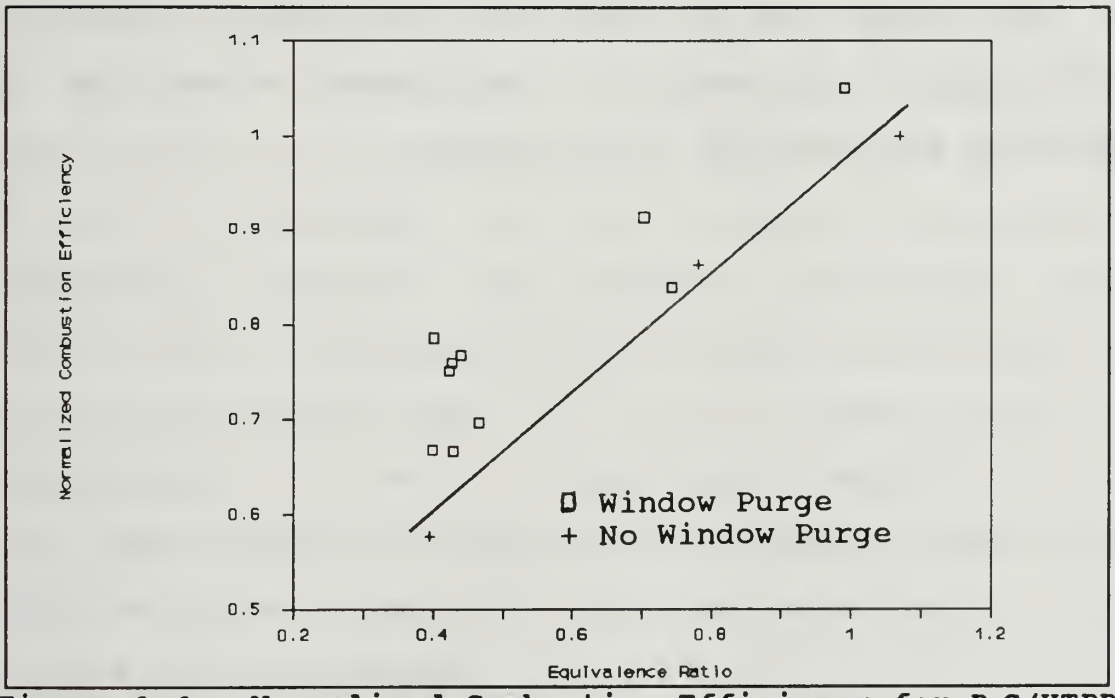

Figure 3.6. Normalized Combustion Efficiency for B_4C/HTPB

As discussed above, the majority of the mass was concentrated in the larger particles, so it is important that these be broken up and consumed or prevented from forming. It is desirable to correlate the unburned fuel directly to combustion efficiency. A mass concentration of the particles in the flow is required. A volume concentration was estimated based on the transmittance, however it was found that beam steering significantly affected the measured transmittance. One would not expect the amount of beam steering to be constant from test to test, so this estimate for volume concentration could not be used. A measurement for transmittance that is not affected by beam steering (such as a large diode and a laser with small beam diameter) is required for a combustion performance correlation with particle size behavior to be derived.

IV. SUMMARY AND CONCLUSIONS

Particle size measurements were taken in the combustion environment of a metallized solid fuel ramjet. These measurements required care in alignment of the Malvern system and in the measurement procedure in order to obtain good results without biasing due to beam steering and secondary reflections. Additional effort is in order to improve the procedure, such that clean windows during the sample period are ensured.

The particle size distributions at the aft end of the fuel grain were generally quadra-modal, with mode peaks at 2, 4, 15, and 25 - 45 microns. At the nozzle entrance the distributions were tri-modal, due to the complete oxidation of the 2 μm particles. $D_{3,2}$ and the size of the largest agglomerates increased with increasing equivalence ratio (grain length), indicating that the longer grains result in more surface agglomeration. $D_{3,2}$ did not change across the mixing chamber as a result of the complete oxidation of the large number of smallest particles, thus balancing the partial oxidation of the larger, but fewer, particles where most of the mass was concentrated.

Combustion efficiency increased with equivalence ratio. A direct correlation of particle size alone with combustion

efficiency was not obvious and may require a more accurate measurement of particle concentration. A combustion temperature above some limiting value may be required for combustion of the particle fragments to occur. This may explain the observed increase in combustion efficiency with equivalence ratio.

Cold air window purge appeared to increase combustion efficiency. This air can enhance both particle breakup and oxidation. This observation implies that hot bypass air may result in significant improvements in combustion efficiency.

Combustion performance may possibly be correlated with the particle size distribution, if the mass concentration of unburned fuel in the combustion chamber can be determined. This will require a measurement of light transmittance through the reacting flow that is not sensitive to beam steering. Thus, five tests will be required for a single flow condition: one test for performance, two tests for particle size distributions and an additional two tests for a light transmittance measurement at each station.

The data base from this investigation was quite small. Expansion of this data base is required to validate the conclusions observed. This should include investigation of the particle size distribution for other air mass fluxes, combustor chamber pressures and inlet air temperatures. Once

this fuel is well documented, other metallized based fuels should be considered.

LIST OF REFERENCES

1. United Technologies/Chemical Systems Division, *The Pocket Ramjet Reader*, 1978.
2. Gany, A., and Netzer, D. W., "Fuel Performance Evaluation for the Solid-Fueled Ramjet," *International Journal of Turbo and Jet Engines*, Vol. 2, 1985.
3. Gany, A., and Netzer, D. W., "Combustion Studies of Metallized Fuels for Solid-Fuel Ramjets," *Journal of Propulsion and Power*, Vol. 2, No. 5, September-October 1986, pp. 423-427.
4. Myers, T. D., "Special Problems of Ramjet with Solid Fuel," *Ramjet and Ramrocket Propulsion Systems for Missiles*, AGARD Lecture Series 136, September 1984.
5. Mady, C. J., Hickey, P. J., and Netzer, D. W., "Combustion Behavior of Solid-Fuel Ramjets," *Journal of Spacecraft and Rockets*, Vol. 15, May-June 1978, pp. 131-132.
6. Williams, F. A., *Combustion Theory*, Addison Wesley Publishing Co., Reading, MA, 1965, pp. 296-305.
7. Laredo, D., and Gany, A., "Combustion Phenomena of Highly Metallized Solid Propellants," *Acta Astronautica*, Vol. 10, 1983, pp. 437-441.

8. King, M. K., "Modeling of Single Particle Boron Combustion," 19th JANNAF Combustion Meeting, CPIA Pub. 366, Vol. II, p. 43. 1982.

9. Karadimitris, A., *The Effects of Metallized Fuel Composition on the Combustion Characteristics of Solid Fuel Ramjets*, Master's Thesis, Naval Postgraduate School, Monterey, CA, December 1986.

10. Paty, Robert P., *Holographic Particle Sizing in Solid Fuel Ramjets*, Master's Thesis, Naval Postgraduate School, Monterey, CA, September 1988.

11. Youngborg, E. D., Pruitt, T. E., Smith, M. J., and Netzer, D. W., "Light Diffraction Particle Size Measurements in Small Solid Propellant Rockets," to be published in *Journal of Propulsion and Power*, November-December 1989.

12. Malvern Instruments, *Malvern Particle Sizer Reference Manual*, Version 3.0, 1986.

13. Naval Weapons Center Technical Paper 6181, *Ablative Insulators for Ramjet Engines Vol. 2: Reinforced Silicone Elastomers as Ablative Insulators*, Baldwin, James C., and Rhein, Robert A., February 1983.

APPENDIX A (TEST 7)

Malvern Instruments MASTER Particle Sizer M6.10 Date 20-09-89 Time 18-57

Source test7 Record 2
Focal length 100

0	0.64	16	739.96
1	306.09	17	546.76
2	521.98	18	826.02
3	475.54	19	692.69
4	358.67	20	441.28
5	412.10	21	419.98
6	484.87	22	515.38
7	541.59	23	623.67
8	596.52	24	720.61
9	397.37	25	844.96
10	742.90	26	822.40
11	627.67	27	731.35
12	424.06	28	482.60
13	396.73	29	437.14
14	520.32	30	506.49
15	696.31	31	585.25

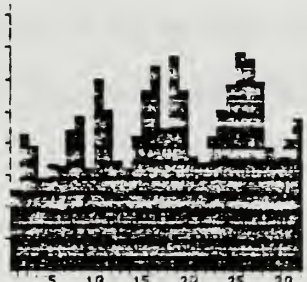

System number 2048 Diode DR487

Malvern Instruments MASTER Particle Sizer M6.10 Date 20-09-89 Time 18-58

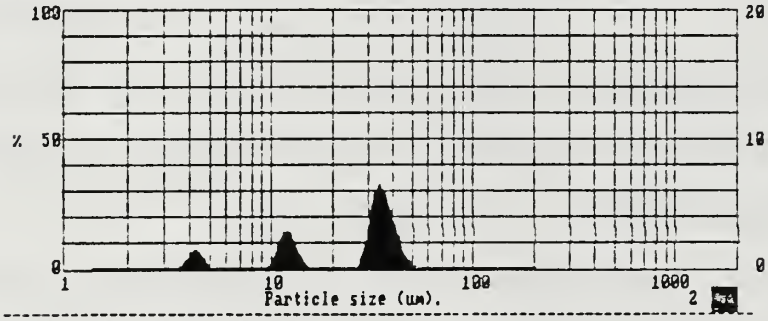

System number 2048 Diode DR487

Malvern Instruments MASTER Particle Sizer M6.10 Date 20-09-89 Time 19-00

Size microns	% under	Size band microns		%	Result source= test7
					Record No. = 2
					Focal length = 100 mm.
188.0	100.0				Experiment type pla
87.2	100.0	188.0	87.2	0.0	Volume distribution
59.5	100.0	87.2	59.5	0.0	Beam length = 6.4 mm.
37.6	79.6	59.5	37.6	20.4	Obscuration =0.6263
23.1	31.8	37.6	23.1	47.8	Volume Conc. = 0.0904 %
14.6	31.8	23.1	14.6	0.0	Log. Diff. =6.15
9.2	27.8	14.6	9.2	0.0	Model indp
5.8	27.8	9.2	5.8	4.1	
3.6	23.6	5.8	3.6	19.2	
2.3	4.4	3.6	2.3	0.0	D(v,0.5) = 32.6 um
1.4	4.4	2.3	1.4	0.0	D(v,0.9) = 40.5 um
0.9	4.4	1.4	0.9	0.0	D(v,1.0) = 10.5 um
0.6	4.4	0.9	0.6	0.0	D(4,3) = 27.7 um
0.4	0.0	0.6	0.4	4.4	D(3,2) = 18.0 um
0.2	-0.0	0.4	0.2	0.0	Span = 0.5
0.1	-0.0	0.2	0.1	0.0	Spec. sur'. area
0.1	-0.0	0.1	0.1	0.0	0.2000 sq.m./cc.

System number 2048 Diode DR487

Malvern Instruments MASTER Particle Sizer M6.10 Date 20-09-89 Time 19-01

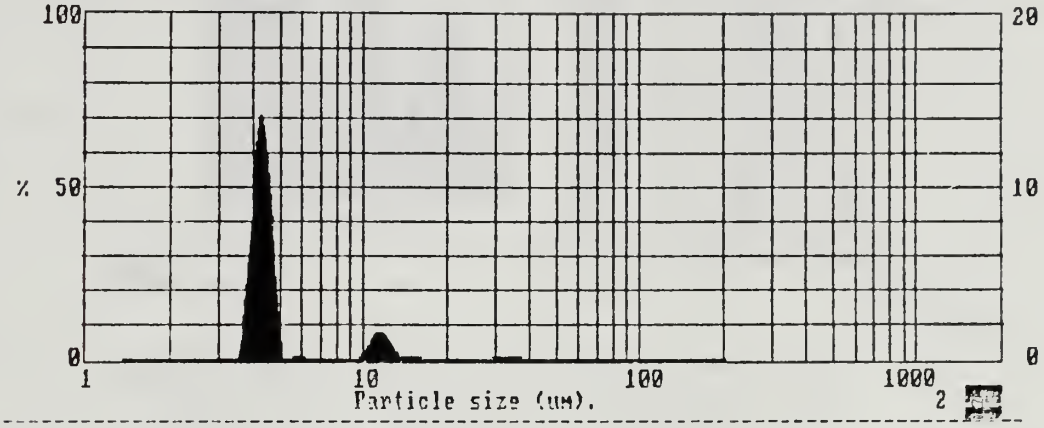

System number 2048 Diode DR487

Malvern Instruments MASTER Particle Sizer M6.10 Date 20-09-89 Time 19-02

Size microns	% under	Size band microns		%	Result source= test7
					Record No. = 2
					Focal length = 100 mm.
188.0	100.0				Experiment type pia
87.2	100.0	188.0	87.2	0.0	Number distribution
53.5	100.0	87.2	53.5	0.0	Beam length = 6.4 mm.
37.6	99.8	53.5	37.6	0.2	Obscuration =0.6359
28.1	98.7	37.6	28.1	1.1	Volume Conc. = 0.0304 %
21.5	98.7	28.1	21.5	0.0	Log. Diff. =6.15
16.7	98.7	21.5	16.7	0.0	Model indp
13.0	97.7	16.7	13.0	1.0	
10.1	87.4	13.0	10.1	10.3	D(v,0.5) = 32.6 um
7.9	87.4	10.1	7.9	0.0	D(v,0.9) = 40.5 um
6.2	87.4	7.9	6.2	0.0	D(v,0.1) = 10.6 um
4.8	87.4	6.2	4.8	0.0	D(4,3) = 27.7 um
3.8	0.0	4.8	3.8	87.4	D(3,2) = 18.0 um
3.0	0.0	3.8	3.0	0.0	Span = 0.9
2.4	0.0	3.0	2.4	0.0	Spec. surf. area
1.9	0.0	2.4	1.9	0.0	0.3524 sq.m./cc.

System number 2048 Diode DR487

APPENDIX B (TEST 9)

Malvern Instruments MASTER Particle Sizer M6.10 Date 20-09-89 Time 19-23

Source test9 Record 2
Focal length 100

0	0.96	16	957.99
1	519.77	17	423.61
2	500.49	18	889.80
3	286.80	19	509.93
4	338.46	20	349.79
5	705.85	21	569.41
6	714.32	22	984.98
7	749.44	23	984.84
8	783.12	24	940.05
9	32.72	25	980.14
10	737.82	26	965.20
11	402.12	27	964.91
12	349.70	28	965.62
13	688.98	29	979.09
14	898.40	30	993.26
15	969.27	31	994.83

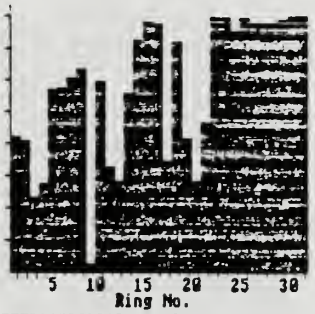

System number 2048 Diode DR487

Malvern Instruments MASTER Particle Sizer M6.10 Date 20-09-89 Time 19-25

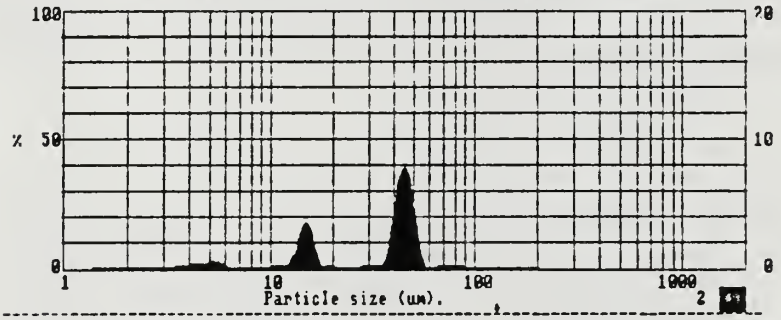

System number 2048 Diode DR487

Malvern Instruments MASTER Particle Sizer M6.10 Date 20-09-89 Time 19-26

Size microns	% under	Size band microns		%
189.0	100.0			
87.2	100.0	189.0	87.2	0.0
53.5	98.7	87.2	53.5	1.3
37.6	32.6	53.5	37.6	66.1
28.1	31.2	37.6	28.1	1.3
[illegible]	[illegible]	28.1	[illegible]	[illegible]
[illegible]	[illegible]	[illegible]	[illegible]	[illegible]
16.7	30.6	21.5	16.7	0.6
13.0	7.9	16.7	13.0	22.7
10.1	6.8	13.0	10.1	1.2
7.9	6.8	10.1	7.9	0.0
6.2	6.7	7.9	6.2	0.0
[illegible]	3.4	6.2	[illegible]	3.3
[illegible]	[illegible]	[illegible]	[illegible]	[illegible]
[illegible]	0.5	[illegible]	[illegible]	0.6
[illegible]	0.5	[illegible]	[illegible]	0.0
[illegible]	0.5	[illegible]	[illegible]	0.0

Result source= test9
Record No. = 2
Focal length = 100 mm.
Experiment type 91a
Volume distribution
Beam length = 6.4 mm.
Obscuration =0.9572
Volume Conc. = 0.3261 %
Log. Diff. =0.20
Model indp

D(v,0.5) = 42.3 um
D(v,[illegible]) = 49.6 um
D(v,[illegible]) = 13.6 um
D(4,3) = 35.0 um
D(3,2) = [illegible] um
Span = 0.9
Spec. surf. area [illegible]

System number 2048 Diode DR487

Malvern Instruments MASTER Particle Sizer M6.10 Date 20-09-89 Time 19-27

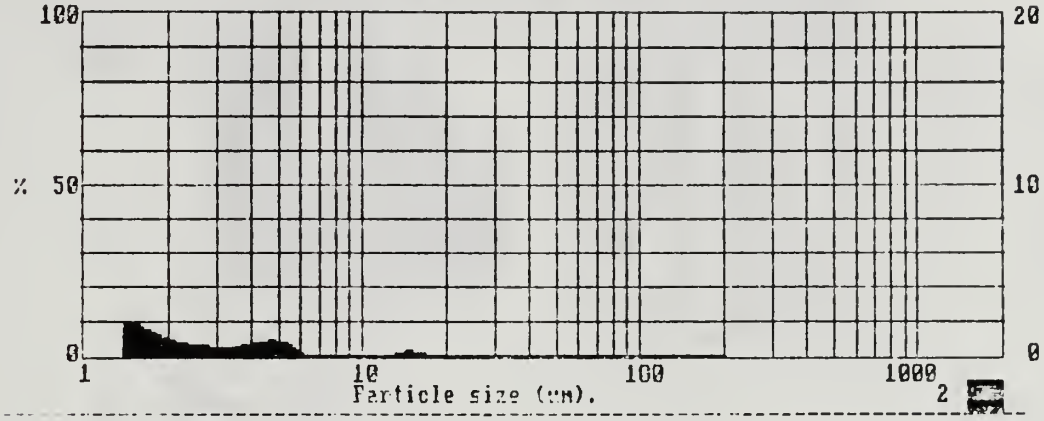

System number 2048 Diode DR487

Malvern Instruments MASTER Particle Sizer M6.10 Date 20-09-89 Time 19-28

Size microns	% under	Size band microns		%	Result source= test9 Record No. = 2
					Focal length = 100 mm.
188.0	100.0				Experiment type fia
87.2	100.0	188.0	87.2	0.0	Number distribution
53.5	100.0	87.2	53.5	0.0	Beam length = 6.4 mm.
37.6	99.8	53.5	37.6	0.2	Obscuration =0.3572
28.1	99.8	37.6	28.1	0.0	Volume Conc. = 0.3361 %
21.5	99.8	28.1	21.5	0.0	Log. Diff. =6.20
16.7	99.8	21.5	16.7	0.0	Model indp
13.0	98.1	16.7	13.0	1.7	
10.1	97.9	13.0	10.1	0.2	D(v,0.5) = 42.3 um
7.9	97.9	10.1	7.9	0.0	D(v,0.9) = 43.6 um
6.2	97.9	7.9	6.2	0.0	D(v,0.1) = 13.6 um
4.8	92.9	6.2	4.8	5.0	D(4,3) = 35.0 um
3.8	87.0	4.8	3.8	5.9	D(3,2) = 23.3 um
3.0	83.4	3.8	3.0	3.6	Span = 0.9
2.4	79.1	3.0	2.4	4.4	Spec. surf. area
1.9	73.0	2.4	1.9	6.1	0.2533 sq.m./cc.

System number 2048 Diode DR487

APPENDIX C (TEST 10)

Malvern Instruments MASTER Particle Sizer M6.10 Date 20-09-89 Time 19-39

Source test10 Record 2
Focal length 100

0	0.96	16	958.32
1	542.36	17	607.18
2	582.35	18	946.94
3	275.38	19	531.09
4	279.18	20	301.87
5	539.78	21	452.93
6	702.59	22	869.73
7	745.94	23	996.56
8	783.54	24	959.14
9	23.79	25	1002.88
10	806.16	26	987.98
11	422.69	27	987.82
12	315.85	28	985.11
13	537.25	29	993.10
14	894.86	30	998.35
15	981.65	31	997.41

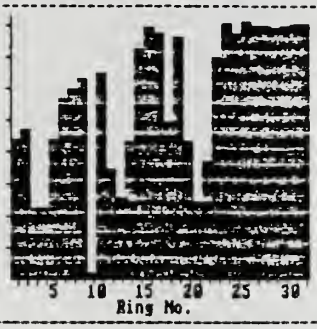

System number 2048 Diode DR487

Malvern Instruments MASTER Particle Sizer M6.10 Date 20-09-89 Time 19-41

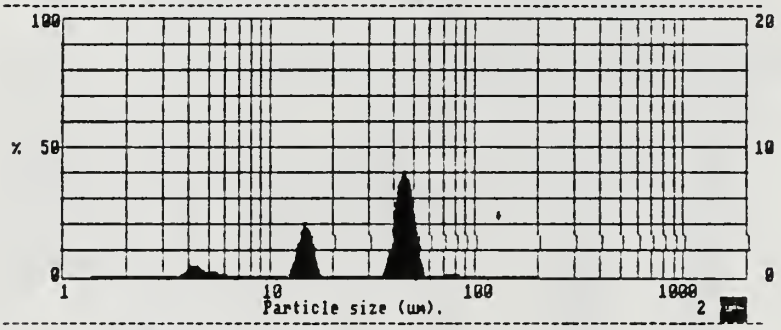

System number 2048 Diode DR487

Malvern Instruments MASTER Particle Sizer M6.10 Date 20-09-89 Time 19-43

Size microns	% under	Size band microns		%	Result source= test10
					Record No. = 2
					Focal length = 100 mm.
188.0	100.0				Experiment type pia
87.2	100.0	188.0	87.2	0.0	Volume distribution
53.5	100.0	87.2	53.5	0.0	Beam length = 6.4 mm.
37.6	32.6	53.5	37.6	67.4	Obscuration =0.3587
28.1	32.6	37.6	28.1	0.0	Volume Conc. = 0.2287 %
21.4	32.6	28.1	21.4	0.0	Log. Diff. =5.96
16.7	32.6	21.4	16.7	0.0	Model indp
13.0	7.6	16.7	13.0	25.0	
10.1	7.6	13.0	10.1	0.0	D(v,0.5) = 42.3 um
7.9	7.6	10.1	7.9	0.0	D(v,0.9) = 83.9 um
6.2	7.6	7.9	6.2	0.0	D(v,1.0) = 87.5 um
4.8	5.9	6.2	4.8	1.7	D(4,3) = 34.6 um
3.8	0.7	4.8	3.8	5.0	D(3,2) = 20.4 um
2.9	0.6	3.8	2.9	0.1	Span = 0.9
2.2	0.6	2.9	2.2	0.0	Uniformity = 0.4
1.9	0.3	2.2	1.9	0.2	Specific surface area = 0.1733 sq.m./cc.

System number 2048 Diode DR487

Malvern Instruments MASTER Particle Sizer M6.10 Date 20-09-89 Time 19-44

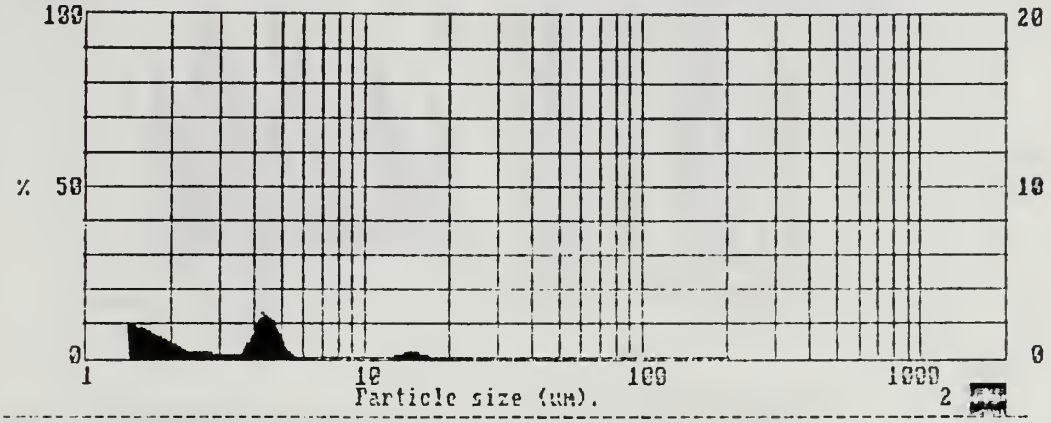

System number 2048 Diode DR487

Malvern Instruments MASTER Particle Sizer M6.10 Date 20-09-89 Time 19-45

Size microns	% under	Size band microns		%	Result source= test10
					Record No. = 2
					Focal length = 100 mm.
189.0	100.0				Experiment type pia
87.2	100.0	189.0	87.2	0.0	Number distribution
53.5	100.0	87.2	53.5	0.0	Beam length = 6.4 mm.
37.6	99.8	53.5	37.6	0.2	Obscuration =0.9587
28.1	99.8	37.6	28.1	0.0	Volume Conc. = 0.3287 %
21.5	99.8	28.1	21.5	0.0	Log. Diff. =5.36
16.7	99.8	21.5	16.7	0.0	Model indp
13.0	97.8	16.7	13.0	2.0	
10.1	97.8	13.0	10.1	0.0	D(v,0.5) = 42.3 um
7.9	97.8	10.1	7.9	0.0	D(v,0.9) = 49.3 um
6.2	97.8	7.9	6.2	0.0	D(v,0.1) = 13.6 um
4.8	95.1	6.2	4.8	2.7	D(4,3) = 34.6 um
3.8	79.0	4.8	3.8	16.2	D(3,2) = 22.4 um
3.0	78.0	3.8	3.0	1.0	Span = 0.8
2.4	76.2	3.0	2.4	1.9	Spec. surf. area
1.9	71.6	2.4	1.9	4.6	0.3089 sq.m./cc.

System number 2048 Diode DR487

APPENDIX D (TEST 11)

Malvern Instruments MASTER Particle Sizer M6.10 Date 20-09-89 Time 18-14

Source test11 Record 2
Focal length 100

0	0.90	16	925.98
1	588.38	17	128.79
2	598.22	18	921.35
3	284.59	19	533.99
4	228.31	20	247.60
5	324.81	21	301.04
6	482.03	22	540.84
7	632.51	23	769.86
8	741.61	24	895.55
9	35.88	25	969.64
10	814.90	26	946.41
11	418.61	27	711.47
12	260.45	28	564.78
13	348.25	29	560.17
14	603.38	30	635.56
15	861.46	31	732.57

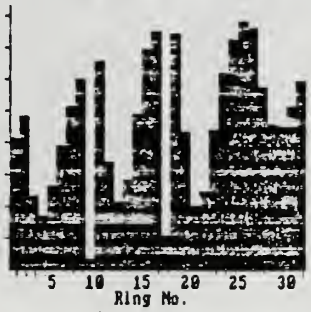

System number 2048 Diode DR487

Malvern Instruments MASTER Particle Sizer M6.10 Date 20-09-89 Time 18-16

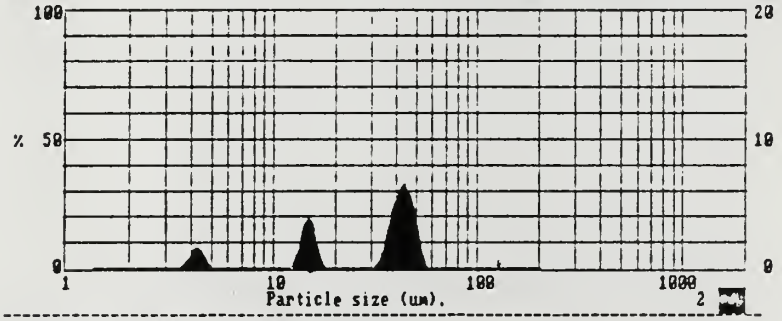

System number 2048 Diode DR487

Malvern Instruments MASTER Particle Sizer M6.10 Date 20-09-89 Time 18-17

Size microns	% under	Size band microns		%	Result source= test11 Record No. = 2
188.0	100.0				Focal length = 100 mm.
87.2	100.0	188.0	87.2	0.0	Experiment type dia
53.6	100.0	87.2	53.6	0.0	Volume distribution
33.0	41.4	53.6	33.0	58.3	Beam length = 6.4 mm.
20.3	34.3	33.0	20.3	7.1	Obscuration =0.3237
12.5	27.2	20.3	12.5	7.1	Volume Conc. = 0.4244 %
7.7	20.1	12.5	7.7	7.1	Log. Diff. =6.29
4.7	13.0	7.7	4.7	7.1	Model indp
2.9	5.1	4.7	2.9	7.9	
1.8	0.0	2.9	1.8	5.1	D(v,0.5) = 39.7 um
					D(v,0.9) = 88.3 um
					= um
					= 32.6 um
					= 20.0 um
					= 1.6
					area
					sq.m./cc.

System number 2048 Diode DR487

Malvern Instruments MASTER Particle Sizer M6.10 Date 20-09-89 Time 20-20

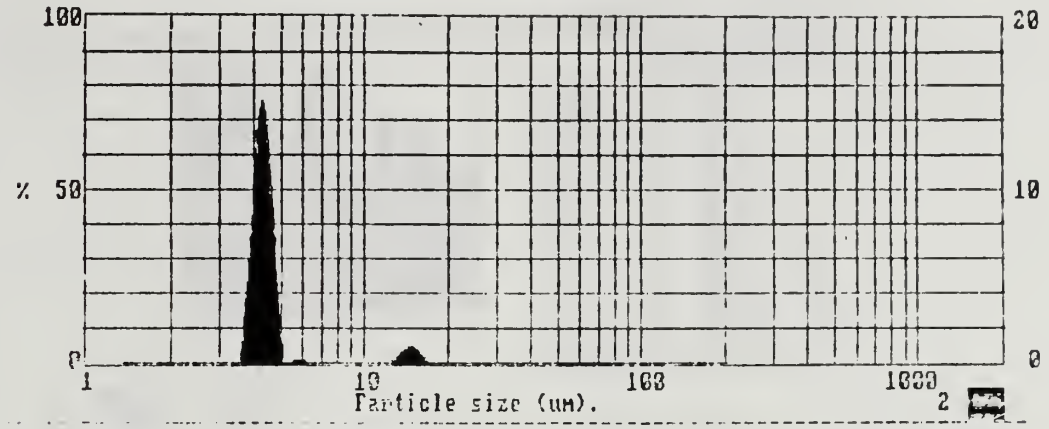

System number 2048 Diode DR487

Malvern Instruments MASTER Particle Sizer M6.10 Date 20-09-89 Time 20:21

Size microns	% under	Size band microns		%	Result source= test1
					Record No. = 2
					Total length = 100 mm.
188.0	100.0				Experiment type fla
87.2	100.0	188.0	87.2	0.0	Number distributio
53.5	100.0	87.2	53.5	0.0	Beam length = 6.4 mm.
37.6	99.5	53.5	37.6	0.5	Obscuration =0.8937
28.1	99.3	37.6	28.1	0.2	Volume Conc. = 0.2244 %
21.5	99.3	28.1	21.5	0.0	Log. Diff. =0.20
16.7	99.3	21.5	16.7	0.0	Model indp
13.0	99.3	16.7	13.0	6.0	
10.1	99.2	13.0	10.1	0.0	D(v,0.5) = 32.7 um
7.9	99.2	10.1	7.9	0.0	D(v,0.3) = 48.3 um
6.2	99.2	7.9	6.2	0.0	D(v,0.1) = 13.3 um
4.8	99.2	6.2	4.8	0.0	D(4,3) = 32.6 um
3.8	-0.0	4.8	3.8	93.2	D(3,2) = 20.0 um
3.0	-0.0	3.8	3.0	0.0	Span = 0.9
2.4	-0.0	3.0	2.4	0.0	Spec. surf. area
1.9	-0.0	2.4	1.9	0.0	0.3233 sq.m./cc.

System number 2048 Diode DR487

APPENDIX E (TEST 12)

Malvern Instruments MASTER Particle Sizer M6.10 Date 20-09-89 Time 19-51

Source test12 Record 2
Focal length 100

0	0.95	16	930.62
1	584.53	17	949.55
2	669.92	18	961.20
3	523.38	19	886.16
4	381.75	20	664.54
5	548.67	21	649.36
6	671.61	22	841.69
7	746.00	23	939.48
8	782.28	24	952.36
9	838.08	25	997.50
10	803.29	26	982.91
11	687.28	27	977.62
12	517.79	28	963.79
13	642.80	29	969.19
14	816.77	30	976.77
15	937.50	31	982.67

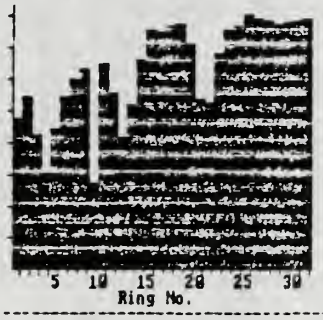

System number 2048 Diode DR487

Malvern Instruments MASTER Particle Sizer M6.10 Date 20-09-89 Time 19-53

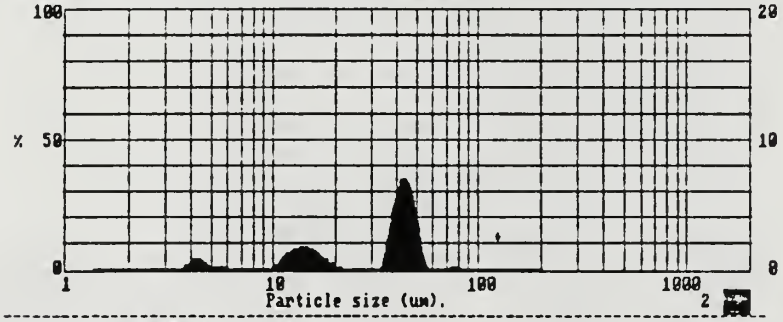

System number 2048 Diode DR487

Malvern Instruments MASTER Particle Sizer M6.10 Date 20-09-89 Time 19-54

Size microns	% under	Size band microns		%	Result source= test12
					Record No. = 2
					Focal length = 100 mm.
					Experiment type pia
					Volume distribution
					Beam length = 6.4 mm.
					Obscuration =0.9552
					Volume Conc. = 0.2705 %
					Log. diff. =5.24
					Model indp
					D(v,0.5) = 40.7 um
					D(v,0.9) = 93.2 um
					D(v,0.1) = 11.6 um
					D(4,3) = 32.6 um
					D(3,2) = 21.5 um
					Span = 0.3
					Spec. surface area
					sq.m./cc.

System number 2048 Diode DR487

Malvern Instruments MASTER Particle Sizer M6.10 Date 20-09-89 Time 19-54

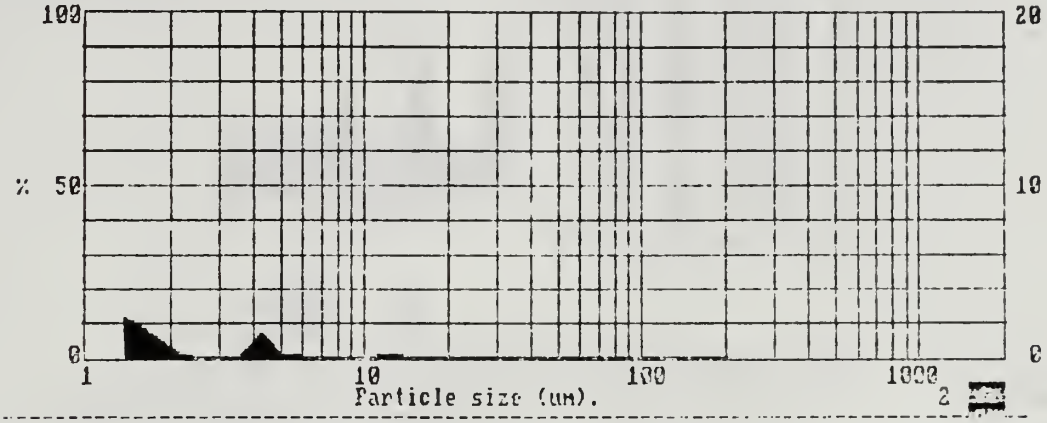

System number 2048 Diode DR187

Malvern Instruments MASTER Particle Sizer M6.10 Date 20 09 89 Time 19-55

Size microns	% under	Size band microns		%	Result source= test12 Record No. = 2
					Focal length = 100 mm.
168.0	100.0				Experiment type pla
87.2	100.0	183.0	87.2	0.0	Number distribution
53.5	100.0	87.2	53.5	0.0	Beam length = 6.4 mm.
37.6	99.9	53.5	37.6	0.1	Obscuration =0.9152
28.1	99.9	37.6	28.1	0.0	Volume Conc. = 0.2795 %
21.5	99.9	28.1	21.5	0.0	Log. Diff. =5.24
16.7	99.8	21.5	16.7	0.1	Model indp
13.0	99.3	16.7	13.0	0.5	
10.1	98.6	13.0	10.1	0.7	D(v,0.5) = 40.7 um
7.9	98.6	10.1	7.9	0.0	D(v,0.9) = 18.6 um
6.2	98.5	7.9	6.2	0.0	D(v,0.1) = 11.5 um
4.8	97.7	6.2	4.8	0.8	D(4,3) = 33.6 um
3.8	93.1	4.8	3.8	4.6	D(3,2) = 21.5 um
3.0	88.6	3.8	3.0	0.4	Span = 0.9
2.4	88.2	3.0	2.4	0.3	Spec. surf. area
1.9	85.8	2.4	1.9	2.5	0.3351 sq.m./cc.

System number 2048 Diode DR487

APPENDIX F (TEST 13)

Malvern Instruments MASTER Particle Sizer M6.10 Date 20-09-89 Time 20-22

Source test13 Record 3
Focal length 100

0	0.88	16	208.74
1	133.93	17	196.92
2	506.16	18	399.64
3	467.08	19	374.05
4	189.63	20	262.90
5	145.51	21	255.72
6	148.28	22	211.23
7	195.49	23	291.11
8	191.41	24	241.17
9	168.12	25	217.54
10	553.74	26	276.77
11	444.24	27	303.11
12	238.41	28	243.36
13	189.48	29	232.59
14	188.47	30	218.49
15	238.56	31	234.31

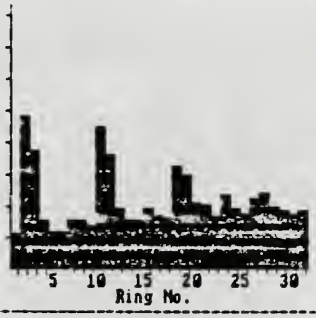

System number 2048 Diode DR487

Malvern Instruments MASTER Particle Sizer M6.10 Date 20-09-89 Time 20-24

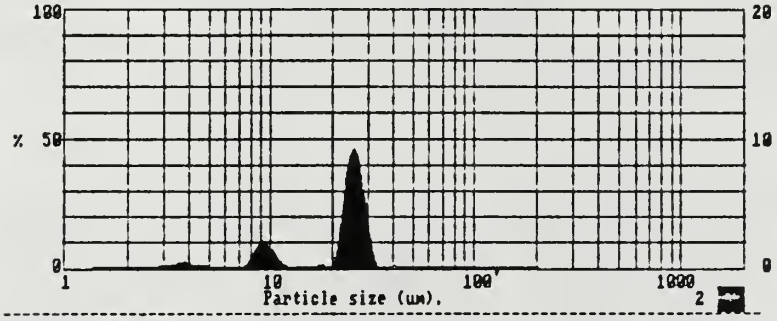

System number 2048 Diode DR487

Malvern Instruments MASTER Particle Sizer M6.10 Date 20-09-89 Time 20-25

Size microns	% under	Size band microns		%	Result source= test13
					Record No. = 3
					Focal length = 100 mm.
188.0	100.0				Experiment type pia
87.2	100.0	188.0	87.2	0.0	Volume distribution
53.5	100.0	87.2	53.5	0.0	Beam length = 5.4 mm.
37.6	99.4	53.5	37.6	0.6	Obscuration =0.8775
28.1	86.7	37.6	28.1	12.7	Volume Conc. = 0.1864 %
21.5	21.1	28.1	21.5	65.6	Log. Diff. =6.16
16.7	20.9	21.5	16.7	0.2	Model indp
[illegible]	[illegible]	[illegible]	[illegible]	[illegible]	
[illegible]	[illegible]	[illegible]	[illegible]	[illegible]	D(v,0.5) = 24.5 um
7.3	1.0	10.1	7.3	13.2	D(v,0.3) = 20.5 um
6.4	0.7	7.3	6.4	0.3	D(v,0.1) = 0.0 um
5.8	0.5	6.4	5.8	0.2	D(4,3) = 22.0 um
[illegible]	[illegible]	[illegible]	[illegible]	[illegible]	D(3,2) = [illegible] um
[illegible]	[illegible]	[illegible]	[illegible]	[illegible]	[illegible] = [illegible]
2.0	0.3	2.4	2.0	1.5	Span = 0.9
1.7	0.0	2.0	1.7	0.3	Uniformity = [illegible]
1.4	0.0	1.7	1.4	0.0	Specific surf. area = [illegible]
[illegible]	0.0	1.4	[illegible]	0.0	Mean SD = [illegible]

System number 2048 Diode DR487

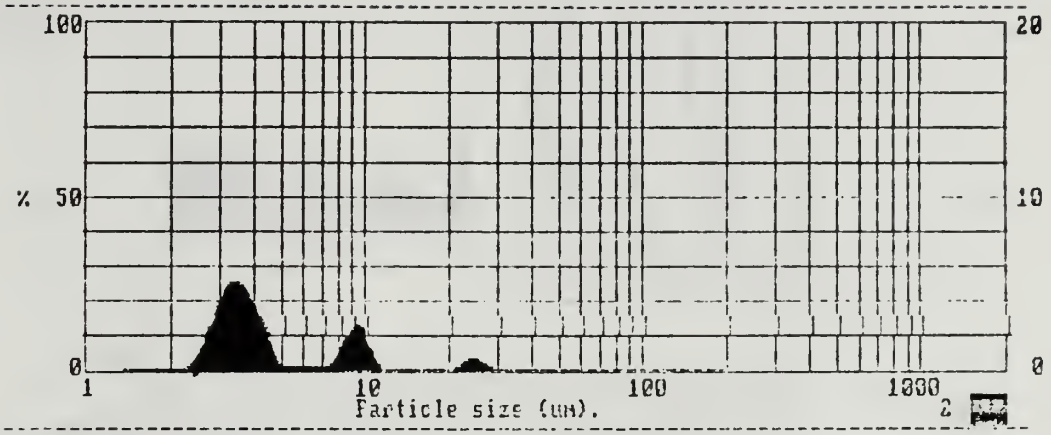

System number 2010 Diode DR407

Malvern Instruments MASTER Particle Sizer M6.10 Date 20-03-89 Time 20-27

Size microns	% under	Size band microns		%	Result source= test13
					Record No. = 3
					Focal length = 100 mm.
188.0	100.0				Experiment type pia
87.2	100.0	188.0	87.2	0.0	Number distribution
[illegible]	[illegible]	87.2	53.5	0.0	Beam length = 6.4 mm.
37.6	100.0	53.5	37.6	0.0	Obscuration =0.8775
28.1	99.6	37.6	28.1	0.4	Volume Conc. = 0.1864 %
21.5	98.4	28.1	21.5	1.2	Log. Diff. =0.16
16.7	95.4	21.5	16.7	3.0	Model indp
13.0	95.4	16.7	13.0	0.0	
10.1	93.0	13.0	10.1	2.4	D(v,0.5) = 24.8 um
7.9	75.3	10.1	7.9	17.7	D(v,0.9) = 28.6 um
6.2	74.4	7.9	6.2	0.9	D(v,0.1) = 9.0 um
4.8	73.0	6.2	4.8	1.4	D(4,3) = 22.0 um
3.8	53.0	4.8	3.8	20.0	D(3,2) = 18.2 um
3.0	15.2	3.8	3.0	37.8	Span = 0.8
2.4	0.2	3.0	2.4	15.0	Spec. surf. area
1.9	0.1	2.4	1.9	0.1	0.3550 sq.m./cc.

System number 2048 Diode DR487

APPENDIX G (TEST 17)

Source test17 Record 1
Focal length 100

0	:	0.96:	16:	265.18:
1	:	365.18:	17:	230.94:
2	:	177.05:	18:	261.81:
3	:	107.24:	19:	221.25:
4	:	87.64:	20:	218.30:
5	:	115.50:	21:	252.04:
6	:	141.39:	22:	277.77:
7	:	176.37:	23:	298.43:
8	:	215.09:	24:	303.89:
9	:	220.54:	25:	345.34:
10	:	161.73:	26:	339.21:
11	:	100.38:	27:	304.45:
12	:	114.69:	28:	307.97:
13	:	147.63:	29:	314.87:
14	:	194.99:	30:	327.24:
15	:	245.75:	31:	318.22:

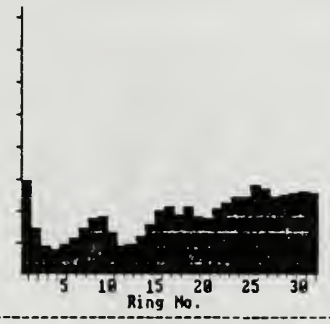

System number 2048 Diode DR487

Malvern Instruments MASTER Particle Sizer M6.10 Date 25-09-89 Time 10-58

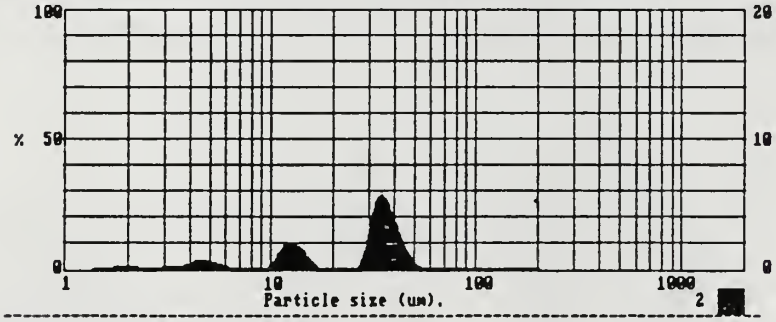

System number 2048 Diode DR487

Malvern Instruments MASTER Particle Sizer M6.10 Date 25-09-89 Time 10-59

Size microns	% under	Size band microns		%	Result source= test17
					Record No. = 1
188.0	100.0				Focal length = 100 mm.
87.2	100.0	188.0	87.2	0.0	Experiment type pia
53.5	100.0	87.2	53.5	0.0	Volume distribution
37.6	77.1	53.5	37.6	22.9	Beam length = 6.4 mm.
28.1	34.0	37.6	28.1	43.0	Obscuration =0.9607
21.5	33.6	28.1	21.5	0.4	Volume Conc. = 0.2445 %
16.7	33.6	21.5	16.7	0.0	Log. Diff. =5.70
13.0	24.1	16.7	13.0	9.5	Model indp
10.1	11.2	13.0	10.1	12.9	
7.9	10.8	10.1	7.9	0.4	D(v,0.5) = 32.5 um
6.2	10.4	7.9	6.2	0.4	D(v,0.9) = 41.6 um
4.8	7.5	6.2	4.8	2.9	D(v,0.1) = 5.7 um
3.8	3.4	4.8	3.8	4.1	D(4,3) = 27.6 um
3.0	2.1	3.8	3.0	1.2	D(3,2) = 17.1 um
2.4	1.8	3.0	2.4	0.4	Span = 1.1
1.9	1.1	2.4	1.9	0.6	Spec. surf. area
					0.4303 sq.m./cc.

System number 2048 Diode DR487

Malvern Instruments MASTER Particle Sizer M6.10 Date 25-09-89 Time 10-53

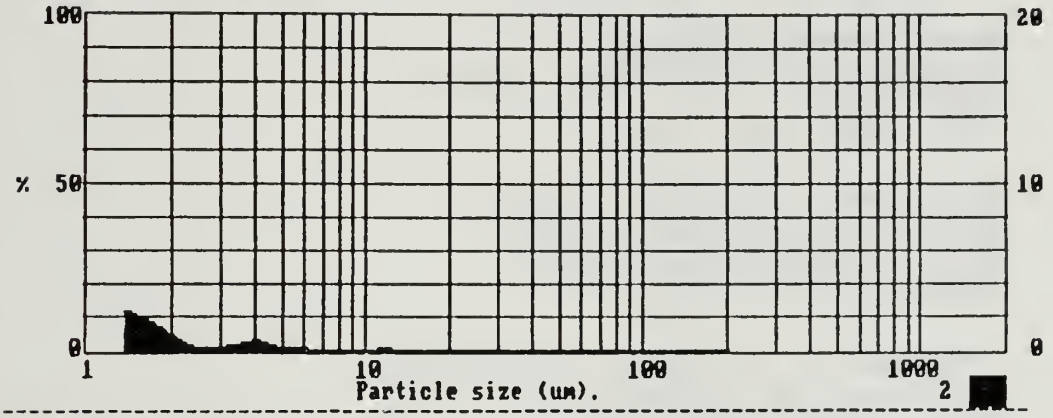

System number 2048 Diode DR487

Malvern Instruments MASTER Particle Sizer M6.10 Date 25-09-89 Time 10-54

Size microns	% under	Size band microns		%	Result source= test17
					Record No. = 1
					Focal length = 100 mm.
188.0	100.0				Experiment type pia
87.2	100.0	188.0	87.2	0.0	Number distribution
53.5	100.0	87.2	53.5	0.0	Beam length = 6.4 mm.
37.6	100.0	53.5	37.6	0.0	Obscuration =0.9607
28.1	99.9	37.6	28.1	0.1	Volume Conc. = 0.2445 %
21.5	99.9	28.1	21.5	0.0	Log. Diff. =5.70
16.7	99.9	21.5	16.7	0.0	Model indp
13.0	99.7	16.7	13.0	0.2	
10.1	99.1	13.0	10.1	0.6	D(v,0.5) = 32.5 um
7.9	99.0	10.1	7.9	0.0	D(v,0.9) = 41.6 um
6.2	98.9	7.9	6.2	0.1	D(v,0.1) = 5.7 um
4.8	97.7	6.2	4.8	1.3	D(4,3) = 27.6 um
3.8	93.9	4.8	3.8	3.8	D(3,2) = 17.1 um
3.0	91.6	3.8	3.0	2.3	Span = 1.1
2.4	90.2	3.0	2.4	1.3	Spec. surf. area
1.9	85.7	2.4	1.9	4.6	0.4303 sq.m./cc.

System number 2048 Diode DR487

INITIAL DISTRIBUTION LIST

1.	Defense Technical Information Center Cameron Station Alexandria, Virginia 22304-6145	2
2.	Naval Postgraduate School Attn: Library, Code 0142 Monterey, CA 93943-5002	2
3.	Naval Weapons Center Airbreathing Propulsion Branch Code 3276 China Lake, CA 93555	3
4.	Department Chairman, Code 67 Department of Aeronautics Naval Postgraduate School Monterey, CA 93943	1
5.	Professor D.W. Netzer, Code 67Nt Department of Aeronautics Naval Postgraduate School Monterey, CA 93943	2
6.	Dr. Taeho Lee, Code 67 Department of Aeronautics Naval Postgraduate School Monterey, CA 93943	1
7.	James Nabity Airbreathing Propulsion Branch Code 3276 Naval Weapons Center China Lake, CA 93555	2

618-567

Thesis
N155
c.1

Nabity
Metallized fuel particle size study in a solid fuel ramjet.

thesN155
Metallized fuel particle size study in a
3 2768 000 87138 8
DUDLEY KNOX LIBRARY